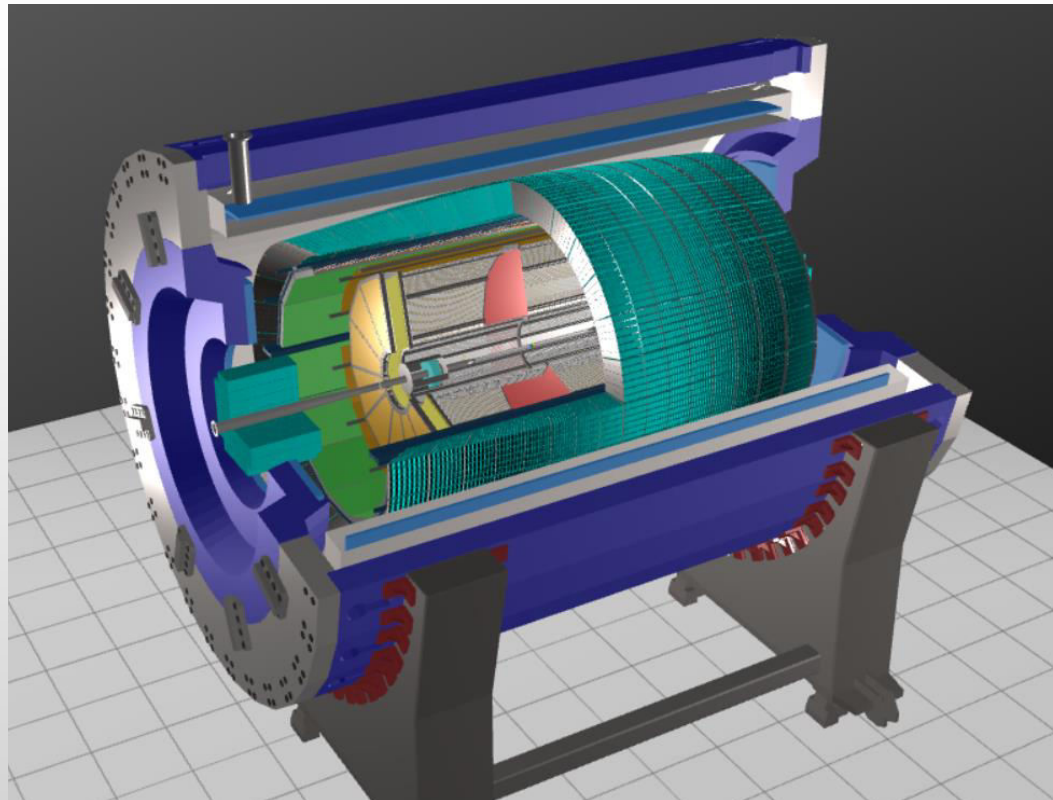


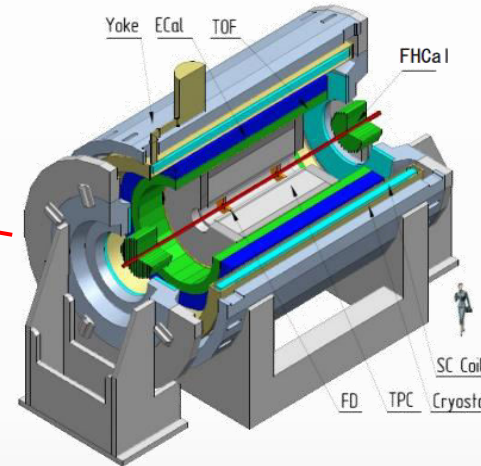
## Status of the MPD detector at NICA

---

V. Riabov for the MPD Collaboration



❖ One of two experiments at NICA collider to study heavy-ion collisions at  $\sqrt{s_{NN}} = 4-11$  GeV



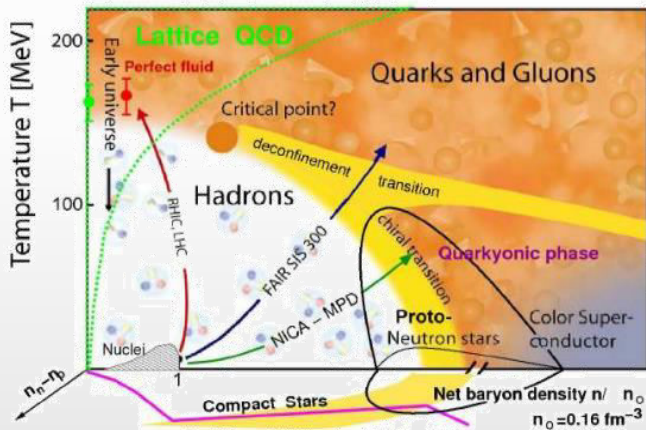
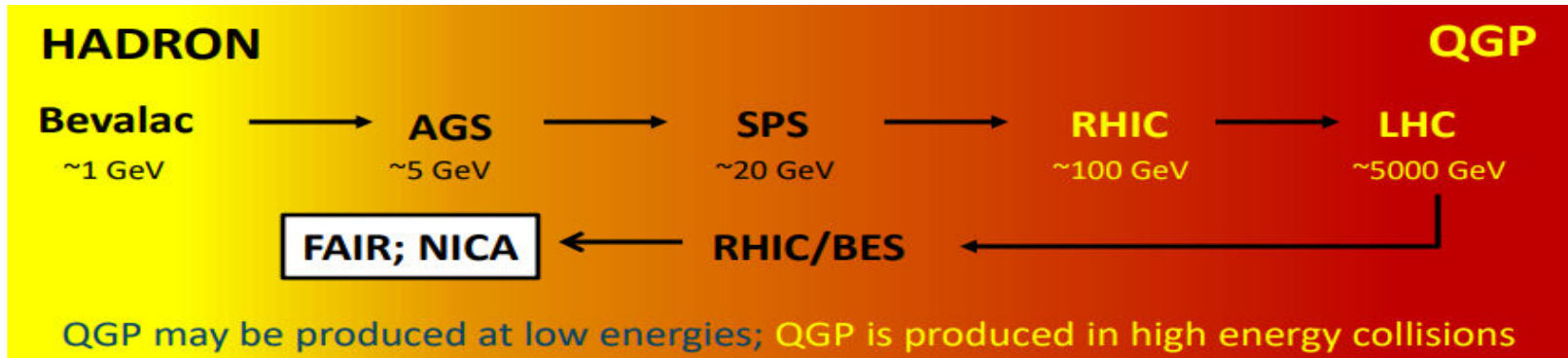
## Stage- I

- TPC:**  $|\Delta\phi| < 2\pi, |\eta| \leq 1.6$
- TOF, EMC:**  $|\Delta\phi| < 2\pi, |\eta| \leq 1.4$
- FFD:**  $|\Delta\phi| < 2\pi, 2.9 < |\eta| < 3.3$
- FHCAL:**  $|\Delta\phi| < 2\pi, 2 < |\eta| < 5$

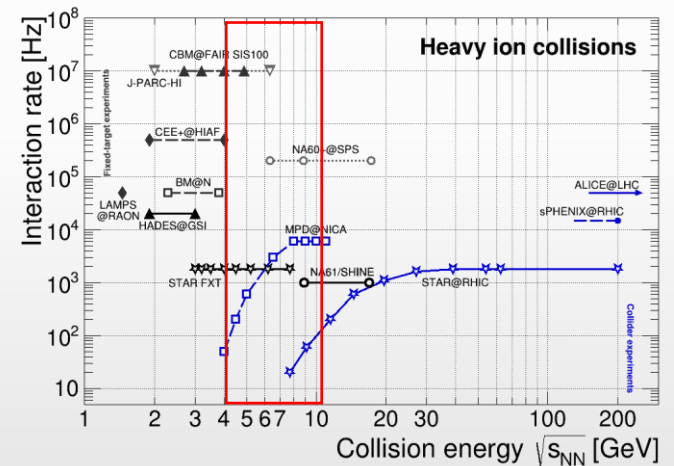
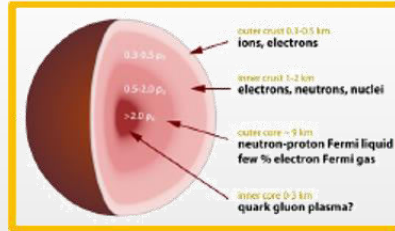
❖ Expected beam configuration in first year(s) of operation:

- ✓ not-optimal beam optics with wide z-vertex distribution,  $\sigma_z \sim 50$  cm
- ✓ reduced luminosity ( $\sim 10^{25}$  is the goal for 2023)  $\rightarrow$  collision rate  $\sim 50$  Hz
- ✓ collision system available with the current sources: C ( $A=12$ ), N ( $A=14$ ), Ar ( $A=40$ ), Fe ( $A=56$ ), Kr ( $A=78-86$ ), Xe ( $A=124-134$ ), Bi ( $A=209$ )
- ✓ First beams: Bi+Bi in 2025

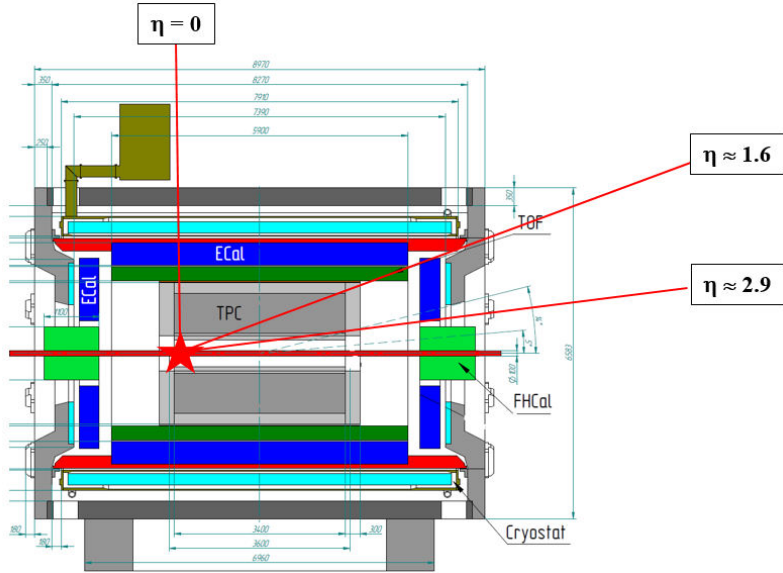
# Relativistic heavy-ion collisions



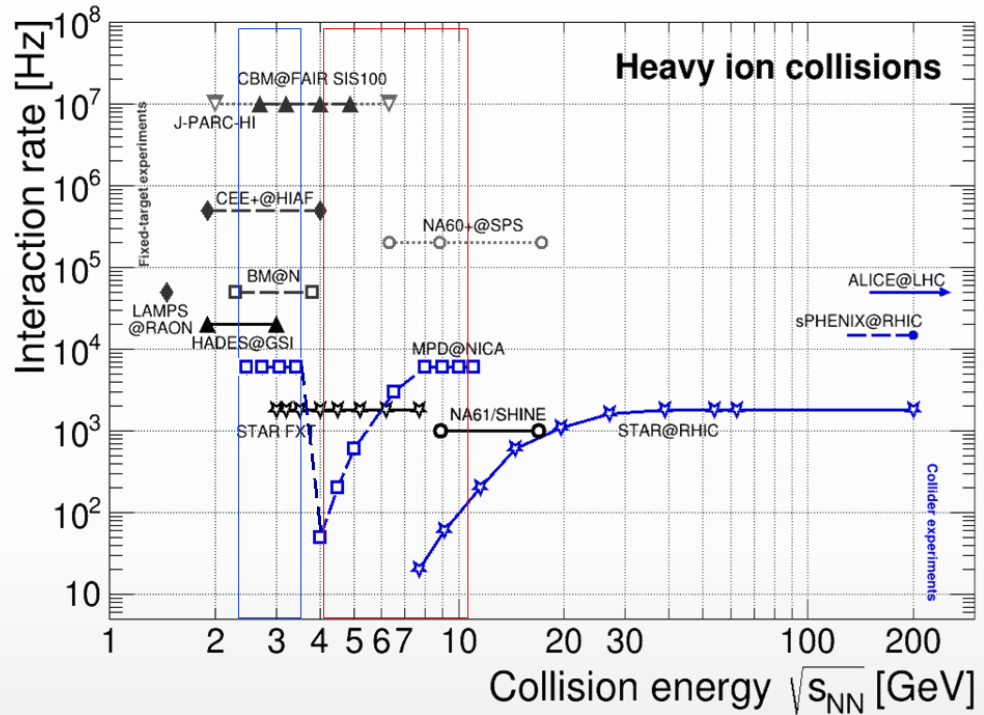
high baryon densities  
→ inner structure of compact stars



- ❖ At  $\mu_B \sim 0$ , smooth crossover (lattice QCD calculations + data)
- ❖ At large  $\mu_B$ , 1<sup>st</sup> order phase transition is expected → QCD critical point
- ❖ BM@N and MPD will study QCD medium at extreme net baryon densities
- ❖ Many ongoing (NA61/Shine, STAR-BES) and future experiments (CBM) in ~ same energy range



E <sub>beam</sub>	$\sqrt{s_{NN}}$ collider mode	$\sqrt{s_{NN}}$ FXT mode	$\eta_{CM}$	CMS coverage
2.0	4	2.4	0.7	-0.7; 0.9 (2.2)
5.5	11	3.5	1.23	-1.23; 0.37 (1.67)



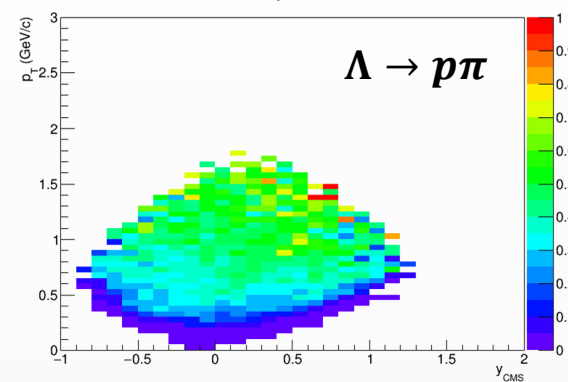
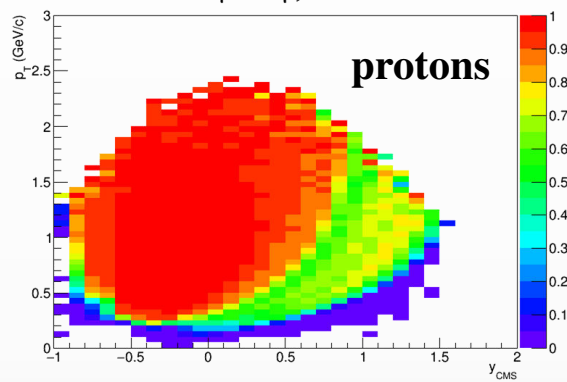
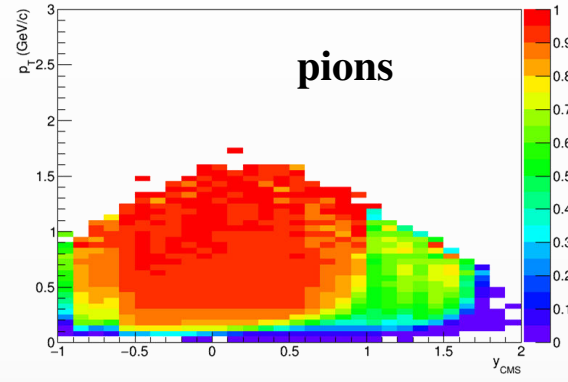
- ❖ Fixed-target mode: one beam + thin wire ( $\sim 100 \mu\text{m}$ ) close to the edge of the MPD central barrel:
  - ✓ extends energy range of MPD to  $\sqrt{s_{NN}} = 2.4\text{-}3.5 \text{ GeV}$  (overlap with HADES, BM@N and CBM)
  - ✓ solves problem of low event rate at lower collision energies (only  $\sim 50 \text{ Hz}$  at  $\sqrt{s_{NN}} = 4 \text{ GeV}$  at design luminosity)
  - ✓ backup start-up solution (too low luminosity, only one beam, etc.)

# Detector performance in FXT mode

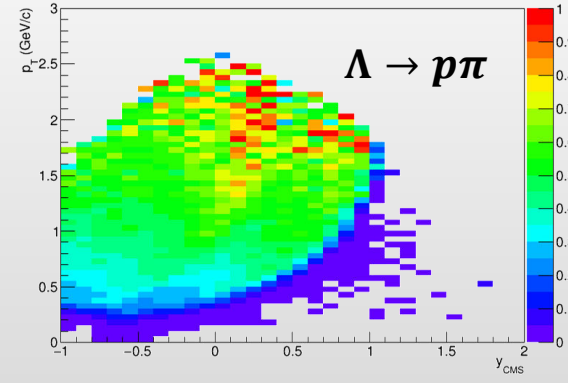
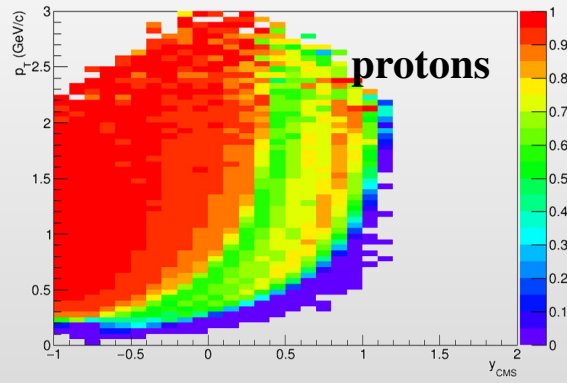
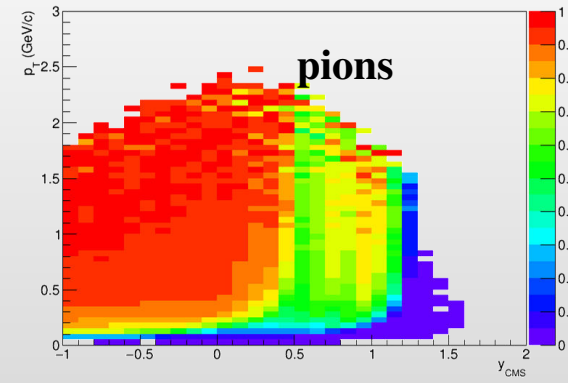
- ❖ Existing trigger system is even more efficient compared with the collider mode (FFD + FHCAL + TOF)
- ❖ MPD detector provides good enough acceptance for identified hadrons at midrapidity ( $y_{\text{CMS}} \sim 0$ ):

✓  $E = 2 \text{ A}\cdot\text{GeV}$

Track selections:  $N_{\text{hits}} > 10$ ;  $\text{DCA} < 2 \text{ cm}$ ; Primary particles ( $R_{\text{production}} < 1 \text{ cm}$ )



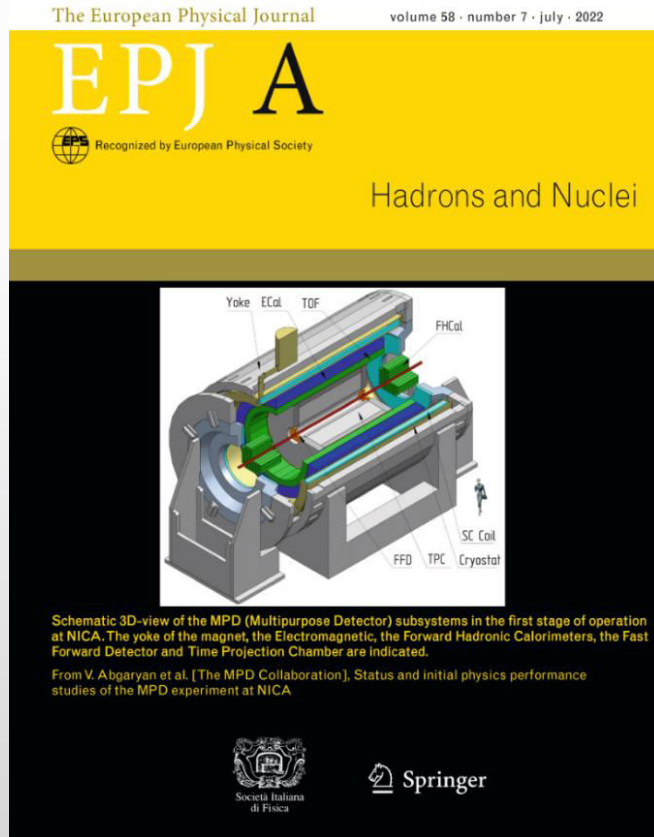
✓  $E = 5.5 \text{ A}\cdot\text{GeV}$



MPD detector is able to run in the fixed-target mode in the default configuration

- ❖ MPD publications: over 200 in total for hardware, software and physics studies (SPIRES)
- ❖ MPD @ conferences: presented at all major conferences in the field
- ❖ First collaboration paper recently published EPJA (~ 50 pages): Eur.Phys.J.A 58 (2022) 7, 140

## Status and initial physics performance studies of the MPD experiment at NICA



Eur. Phys. J. A manuscript No.  
(will be inserted by the editor)

### Status and initial physics performance studies of the MPD experiment at NICA

The MPD Collaboration<sup>1</sup>  
<sup>1</sup>The full list of Collaboration Members is provided at the end of the manuscript

Received: April 20, 2022 / Accepted: date

Abstract: The Nuclotron-based Ion Collider Facility (NICA) is under construction at the Joint Institute for Nuclear Research (JINR), with commissioning of the facility expected in late 2022. The Multi-Purpose Detector (MPD) has been designed to operate at NICA and its components are currently in production. The detector is expected to be ready for data taking with the first beams from NICA. This document provides an overview of the landscape of the investigation of the QCD phase diagram in the region of maximum baryon density, where NICA and MPD will be able to provide significant and unique input. It also provides a detailed description of the MPD set-up, including its various subsystems as well as its support and computing infrastructures. Selected performance studies for particular physics measurements at MPD are presented and discussed in the context of existing data and theoretical expectations.	<ul style="list-style-type: none"> <li>1.1 The Inner Tracking System . . . . . 22</li> <li>1.2 The muon-like Detector . . . . . 23</li> <li>1.3 The Cosmic-Ray Detector . . . . . 23</li> <li>1.4 Infrastructure and support systems . . . . . 24</li> <li>1.5 MPD Hall . . . . . 25</li> <li>1.5.1 Mechanical, installation, and support structure . . . . . 25</li> <li>1.5.2 Support systems . . . . . 26</li> <li>1.5.3 Electronics . . . . . 26</li> <li>1.5.4 Slow Control System . . . . . 26</li> <li>1.5.5 Data Acquisition . . . . . 26</li> <li>2 Software development and computing resources for the MPD experiment . . . . . 27</li> <li>2.1 Software . . . . . 27</li> <li>2.2 Computing . . . . . 27</li> <li>2.3 Preparation for data taking . . . . . 28</li> <li>3 Description of physics feasibility studies . . . . . 28</li> <li>3.1 Centrality determination . . . . . 29</li> <li>3.2 Bulk properties: hadron spectra, yields and ratios . . . . . 31</li> <li>3.3 Particle reconstruction . . . . . 33</li> <li>3.3.1 <math>d, A</math> and <math>z</math>-reconstruction . . . . . 33</li> <li>3.3.2 <math>u, s</math> and <math>J/\psi</math>-reconstruction . . . . . 35</li> <li>3.4 Reconstruction of resonances . . . . . 35</li> <li>3.5 Electromagnetic probe . . . . . 37</li> <li>3.6 Anisotropic flow . . . . . 40</li> <li>3.7 Event-by-event <math>u</math>-quarks and <math>u</math>-like baryons . . . . . 42</li> <li>3.8 Conclusions . . . . . 43</li> <li>4 Acknowledgements . . . . . 45</li> </ul>
---	---

**Contents**

1 Introduction . . . . . 1	1
1.1 Brief survey of the MPD physics goals . . . . . 4	4
1.2 Hadronometry . . . . . 4	4
1.3 Anisotropic flow measurements . . . . . 5	5
1.4 Intensity interferometry . . . . . 7	7
1.5 Resonance . . . . . 7	7
1.6 Short-lived resonances . . . . . 8	8
1.7 Electromagnetic probe . . . . . 10	10
1.8 MPD apparatus . . . . . 11	11
1.8.1 Magnet . . . . . 12	12
1.8.2 Time Projection Chamber . . . . . 13	13
1.8.3 Fast Forward Detector . . . . . 15	15
1.8.4 Electromagnetic Calorimeter . . . . . 16	16
1.8.5 Forward Hadronic Calorimeter . . . . . 17	17
1.8.6 Fast Forward Detector . . . . . 21	21
1.8.7 Plans for additional detectors . . . . . 21	21

**1 Introduction**

The Multi-Purpose Detector (MPD) is one of the two dedicated heavy-ion collision experiments of the Nuclotron-based Ion Collider Facility (NICA), one of the flagship projects, planned to come into operation at the Joint Institute for Nuclear Research (JINR) in 2022. Its main scientific purpose is to search for novel phenomena in the baryon-rich region of the QCD phase diagram by means of colliding heavy nuclei in the energy range of  $4 \text{ GeV} \leq \sqrt{s_{NN}} \leq 11 \text{ GeV}$ .

**G. Feofilov, A. Aparin**

## Global observables

- Total event multiplicity
- Total event energy
- Centrality determination
- Total cross-section measurement
- Event plane measurement at all rapidities
- Spectator measurement

**V. Kolesnikov, Xianglei Zhu**

## Spectra of light flavor and hypernuclei

- Light flavor spectra
- Hyperons and hypernuclei
- Total particle yields and yield ratios
- Kinematic and chemical properties of the event
- Mapping QCD Phase Diag.

**K. Mikhailov, A. Taranenko**

## Correlations and Fluctuations

- Collective flow for hadrons
- Vorticity,  $\Lambda$  polarization
- E-by-E fluctuation of multiplicity, momentum and conserved quantities
- Femtoscopy
- Forward-Backward corr.
- Jet-like correlations

**D. Peresunko, Chi Yang**

## Electromagnetic probes

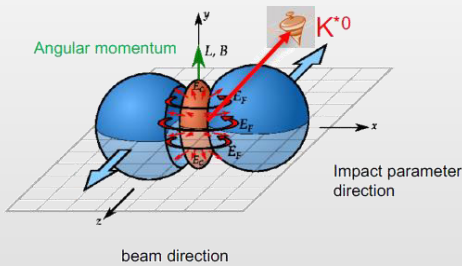
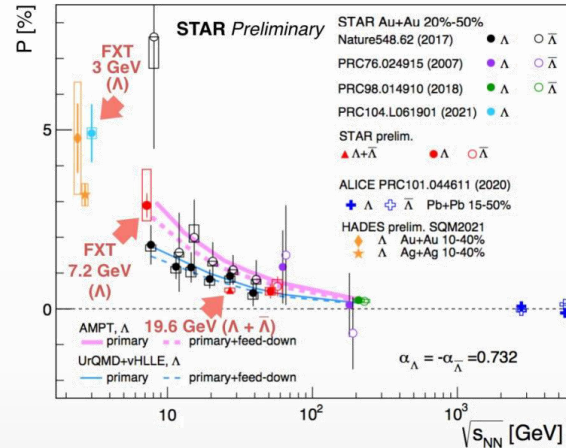
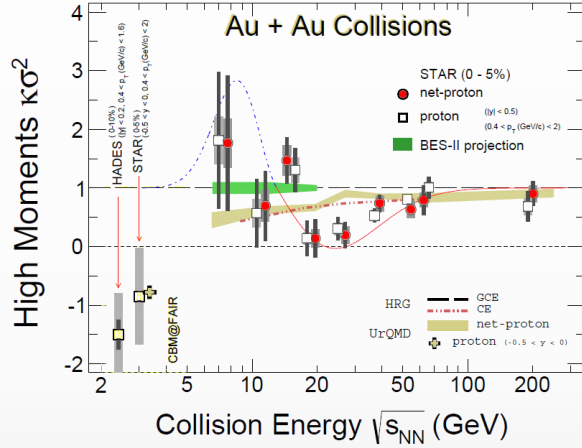
- Electromagnetic calorimeter meas.
- Photons in ECAL and central barrel
- Low mass dilepton spectra in-medium modification of resonances and intermediate mass region

**Wangmei Zha, A. Zinchenko**

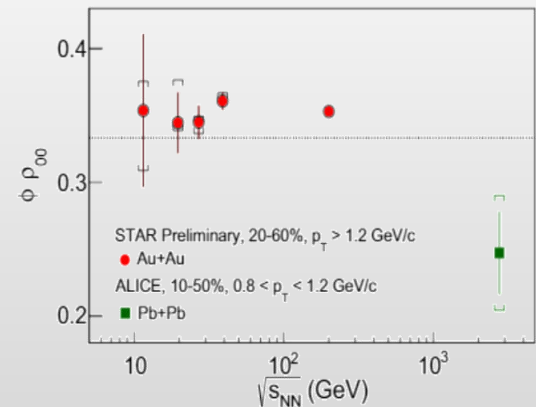
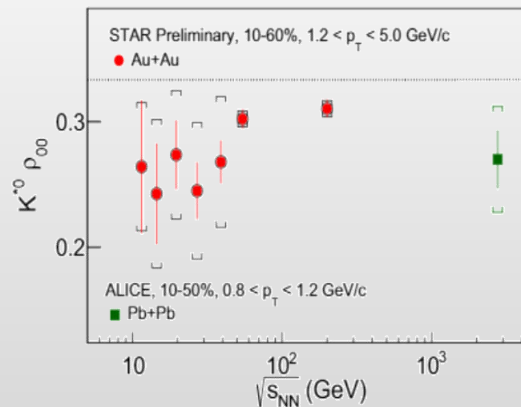
## Heavy flavor

- Study of open charm production
- Charmonium with ECAL and central barrel
- Charmed meson through secondary vertices in ITS and HF electrons
- Explore production at charm threshold

- ❖ Critical fluctuations for (net)proton/kaon multiplicity distributions
- ❖ Global hyperon polarization in mid-central A+A collisions ( $\Lambda$ ,  $\Xi$ ,  $\Omega$ )
- ❖ Spin alignment of vector mesons ( $K^*(892)$ ,  $\phi(1020)$ )



$$\frac{dN}{d\cos\theta} = N_0 [1 - \rho_{0,0} + \cos^2\theta (3\rho_{0,0} - 1)]$$



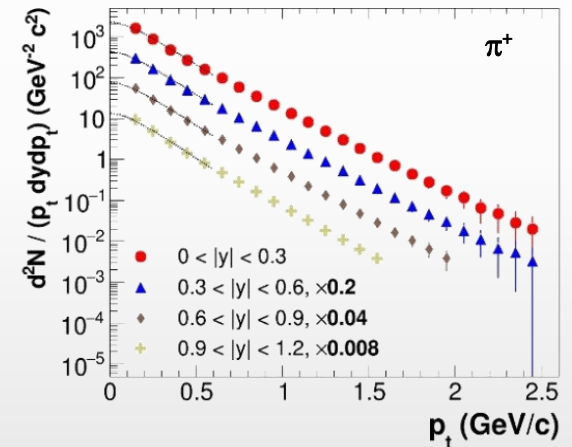
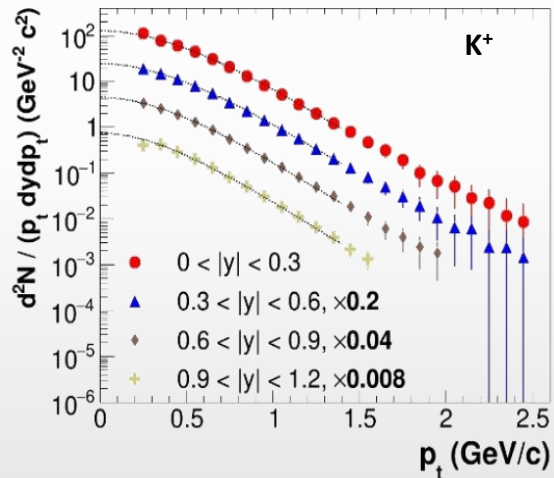
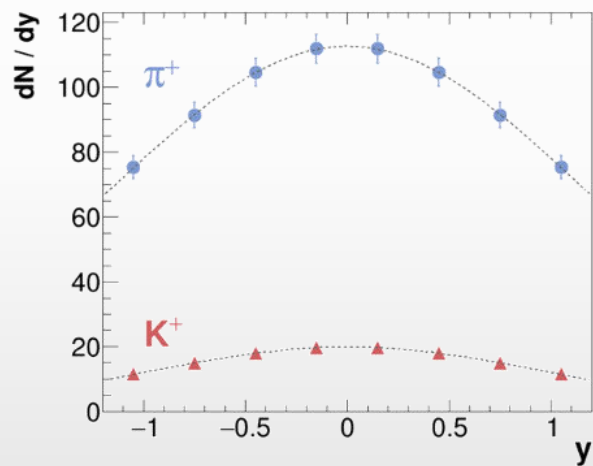
Task for the MPD: extra points in the energy range 4-11 GeV with small uncertainties



- ❖ Probe freeze-out conditions, collective expansion, hadronization mechanisms, strangeness production (“horn” for  $K/\pi$ ), parton energy loss, etc. with particles of different masses, quark contents/counts
- ❖ Charged hadrons: large and uniform acceptance + excellent PID capabilities of TPC and TOF

0-5% central AuAu@9 GeV (PHSD), 5 M events  $\rightarrow$  full event/detector simulation and reconstruction

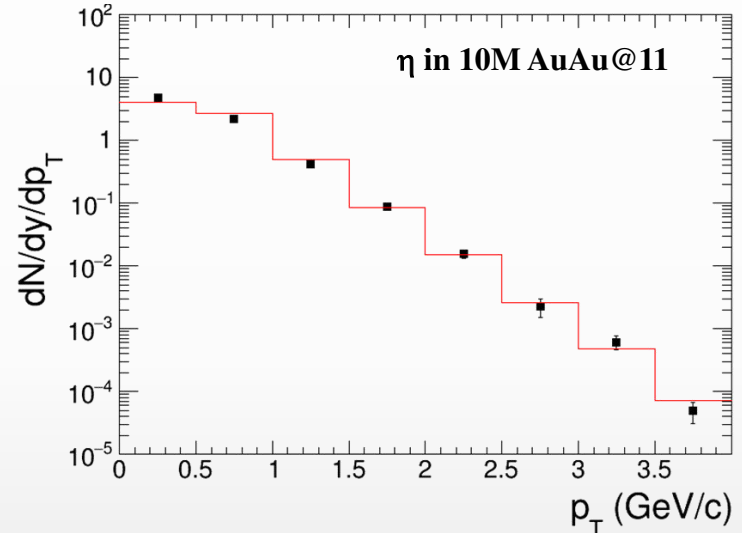
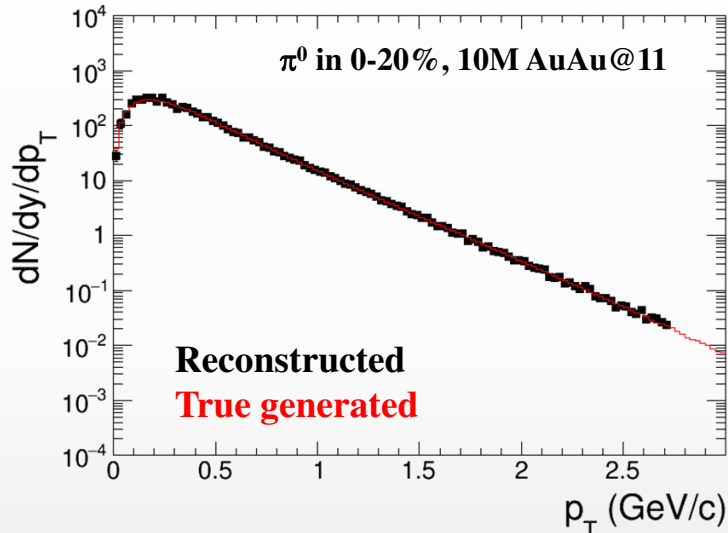
Phys.Part.Nucl. 53 (2022) 2, 203-206



- ✓ sample  $\sim 70\%$  of the  $\pi/K/p$  production in the full phase space
- ✓ hadron spectra are measured from  $p_T \sim 0.1$  GeV/c

- ❖ Neutral mesons ( $\pi^0$ ,  $\eta$ ,  $K_s$ ,  $\omega$ ,  $\eta'$ ): ECAL reconstruction + photon conversion method (PCM)

AuAu@11 GeV (UrQMD), 10M events  $\rightarrow$  full event/detector simulation and reconstruction



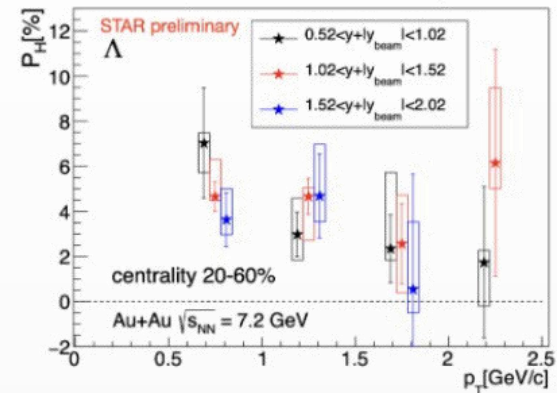
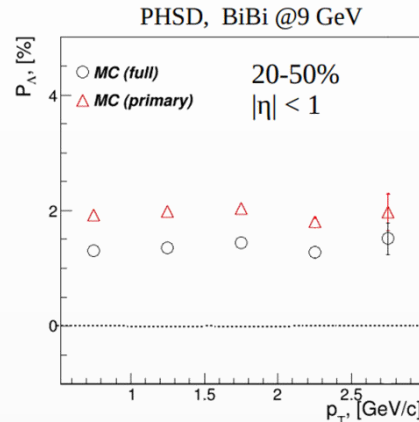
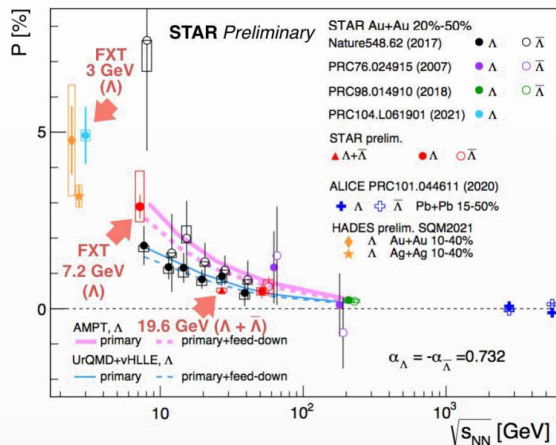
- ✓ extend  $p_T$  ranges of charged particle measurements
- ✓ different systematics

MPD will be able to measure differential production spectra, integrated yields and  $\langle p_T \rangle$ , particle ratios for a wide variety of identified hadrons ( $\pi$ ,  $K$ ,  $\eta$ ,  $\omega$ ,  $p$ ,  $\eta'$ )

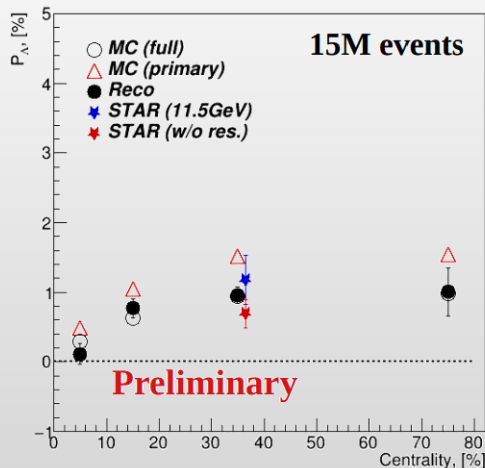
First measurements will be possible with a few million sampled heavy-ion events

# Hyperon global polarization

- ❖ BiBi@9.2 GeV (PHSD), 15 M events → full event/detector simulation and reconstruction
- ❖ Global hyperon polarization (thermodynamical Becattini approach [1]) by the event generator → reproduce at generator level basic features measured by STAR



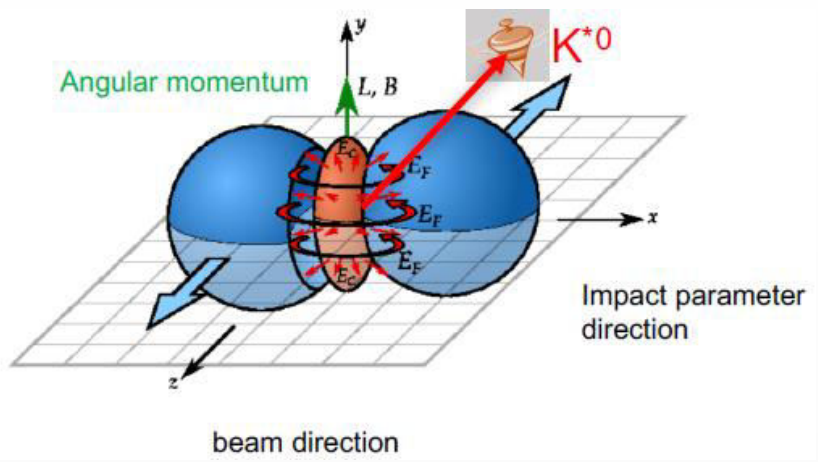
- ❖ Reconstruction of  $\Lambda$  global polarization, work in progress, BiBi@9.2 GeV:



- ❖ Analysis performed using ‘Polarization wagon’ of the Analysis Train
- ❖ Measured polarization is consistent with the generated one
- ❖ First global polarization measurements for  $\Lambda/\bar{\Lambda}$  will be possible with ~ 10M data sampled events

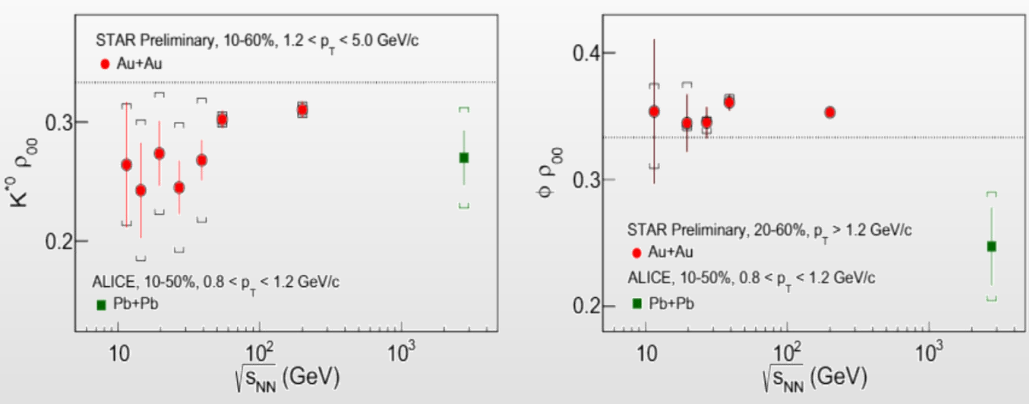
[1] F. Becattini, V. Chandra, L. Del Zanna, E. Grossi, Ann. Phys. 338 (2013) 32

Non-central heavy-ion collisions:



- ❖ Light quarks can be polarized by  $|\vec{J}|$  and  $|\vec{B}|$
- ❖ If vector mesons are produced via recombination their spin may align
- ❖ Quantization axis:
  - ✓ normal to the production plane (momentum of the vector meson and the beam axis)
  - ✓ normal to the event plane (impact parameter and beam axis)
- ❖ Measured as anisotropies:

NPA 1005 (2021) 121733



$$\frac{dN}{d\cos\theta} = N_0 [1 - \rho_{0,0} + \cos^2\theta (3\rho_{0,0} - 1)]$$

$\rho_{0,0}$  is a probability for vector meson to be in spin state = 0  $\rightarrow \rho_{0,0} = 1/3$  corresponds to no spin alignment

- ❖ Measurements at RHIC/LHC challenge theoretical understanding  $\rightarrow \rho_{0,0}$  can depend on multiple physics mechanisms (vorticity, magnetic field, hadronization scenarios, lifetimes and masses of the particles)

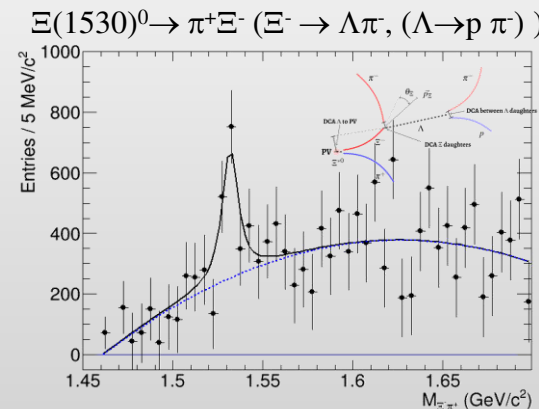
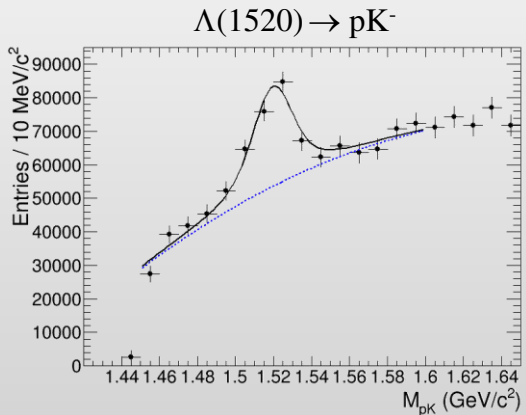
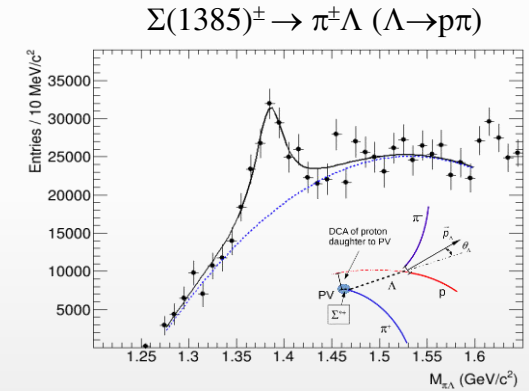
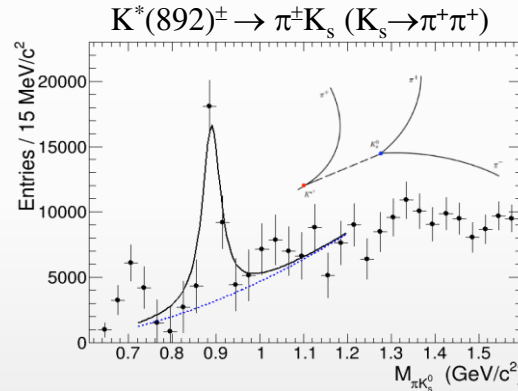
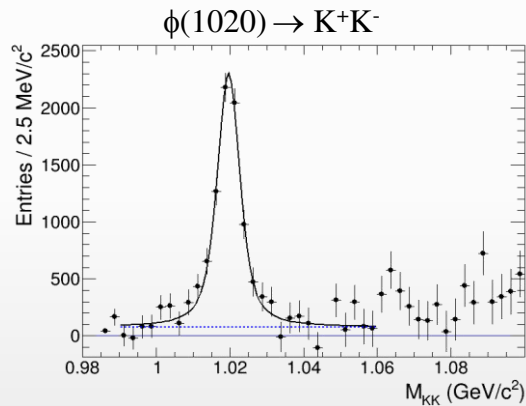
- ❖ Resonances probe reaction dynamics and particle production mechanisms vs. system size and  $\sqrt{s_{NN}}$ :
  - ✓ hadron chemistry and strangeness production, lifetime and properties of the hadronic phase, spin alignment of vector mesons, flow etc.

increasing lifetime  $\longrightarrow$

	$\rho(770)$	$K^*(892)$	$\Sigma(1385)$	$\Lambda(1520)$	$\Xi(1530)$	$\phi(1020)$
$c\tau$ (fm/c)	1.3	4.2	5.5	12.7	21.7	46.2
$\sigma_{\text{rescatt}}$	$\sigma_{\pi}\sigma_{\pi}$	$\sigma_{\pi}\sigma_K$	$\sigma_{\pi}\sigma_{\Lambda}$	$\sigma_K\sigma_p$	$\sigma_{\pi}\sigma_{\Xi}$	$\sigma_K\sigma_K$

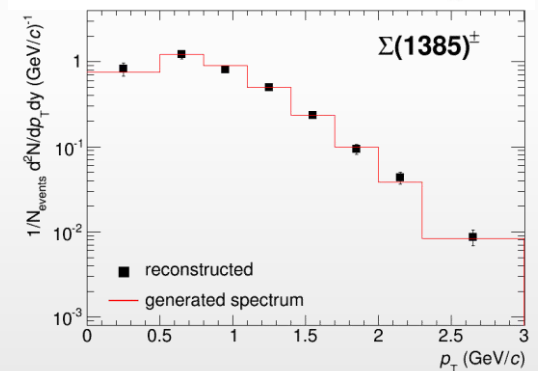
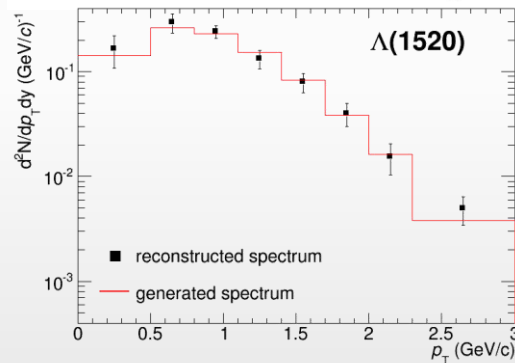
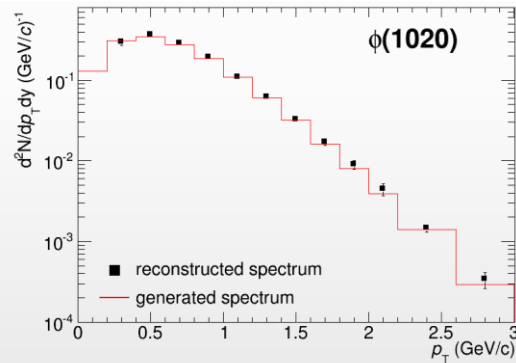
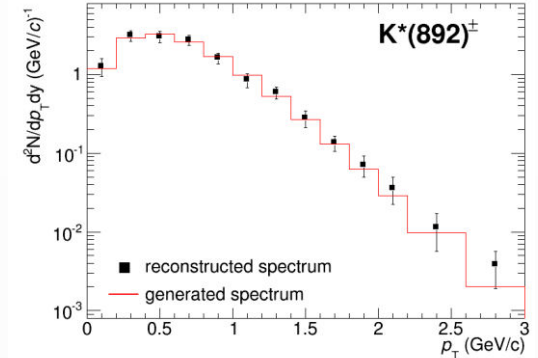
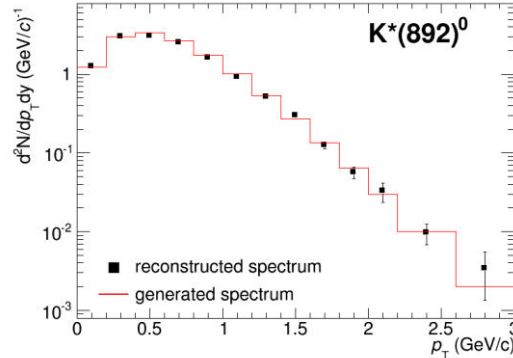
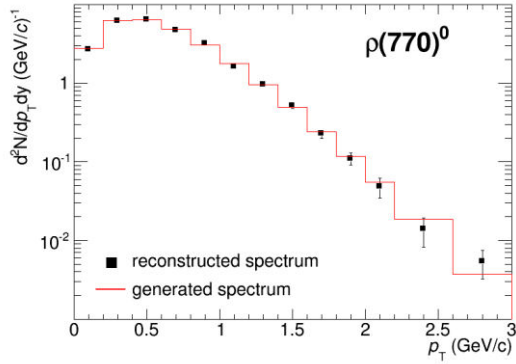
- ❖ BiBi@9.2 GeV (UrQMD) after mixed-event background subtraction:

*Phys.Scripta* 96 (2021) 6, 064002



- ✓ MPD is capable of reconstructing the resonance peaks in the invariant mass distributions using combined charged hadron identification in the TPC and TOF
- ✓ decays with weakly decaying daughters require additional second vertex and topology cuts for reconstruction

❖ Full chain simulation and reconstruction,  $p_T$  ranges are limited by the possibility to extract signals,  $|y| < 1$

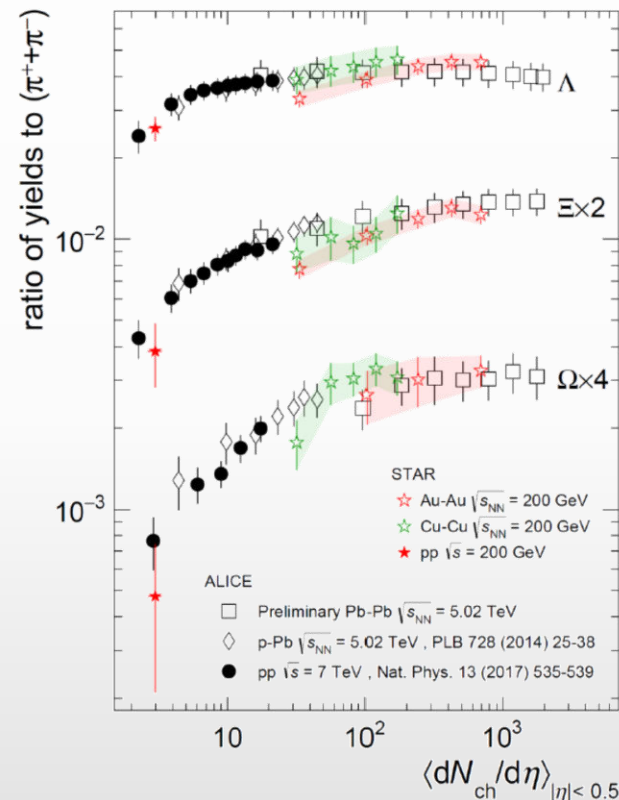
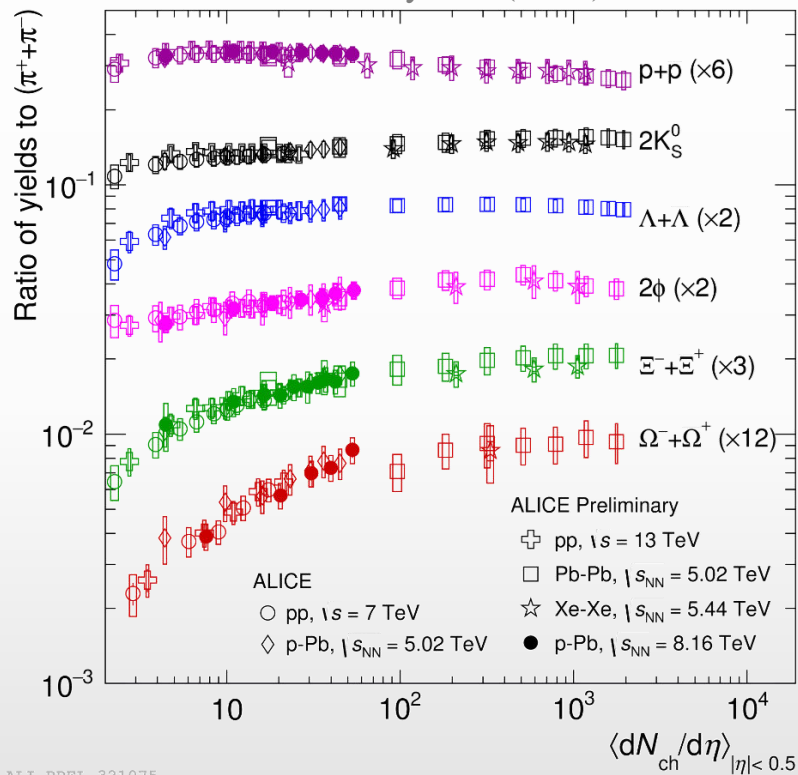


- ❖ Reconstructed spectra match the generated ones within uncertainties
- ❖ First measurements for resonances will be possible with accumulation of  $\sim 10^7$  Bi+Bi events
- ❖ Measurements are possible starting from  $\sim$  zero momentum  $\rightarrow$  sample most of the yield
- ❖ Measurements of  $\Xi(1530)^0$  are very statistics hungry

# Strangeness production: pp, p-A, A-A

- ❖ Since the mid 80s, strangeness enhancement is considered as a signature of the QGP formation
- ❖ Experimentally observed in heavy-ion collisions at AGS, SPS, RHIC and LHC energies

Nature Phys. 13 (2017) 535

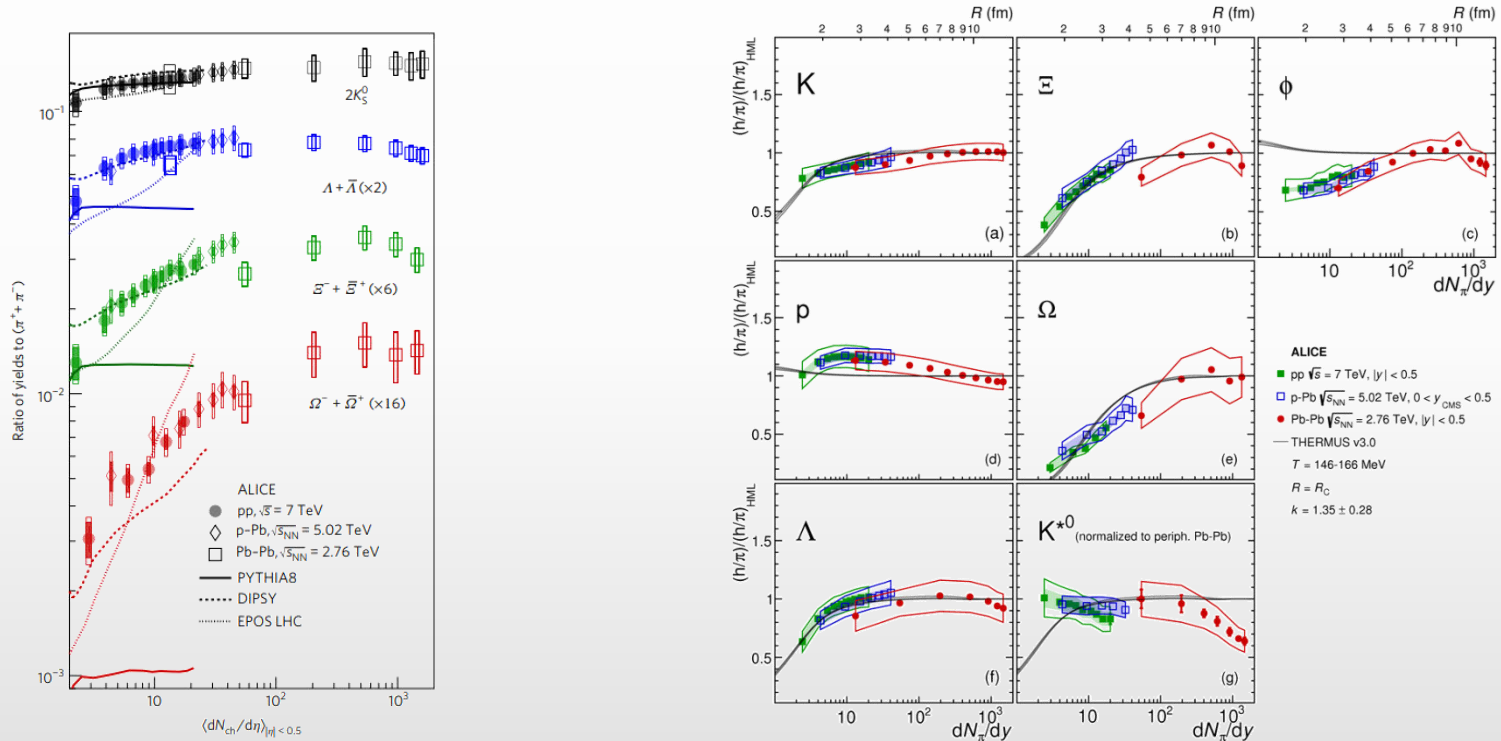


- ❖ Smooth evolution vs. multiplicity in pp, p-A and A-A collisions at LHC energies
- ❖ Strangeness enhancement increases with strangeness content and particle multiplicity
- ❖ STAR @ RHIC measurements in pp, A-A are in agreement with ALICE @ LHC at similar  $\langle dN_{ch}/d\eta \rangle$

- ❖ Origin of the strangeness enhancement in small/large systems is still under debate:
  - ✓ strangeness enhancement in QGP contradicts with the observed collision energy dependence
  - ✓ strangeness suppression in pp within canonical suppression models reproduces most of results except for  $\phi(1020)$

Nature Physics volume 13, pages535–539 (2017)

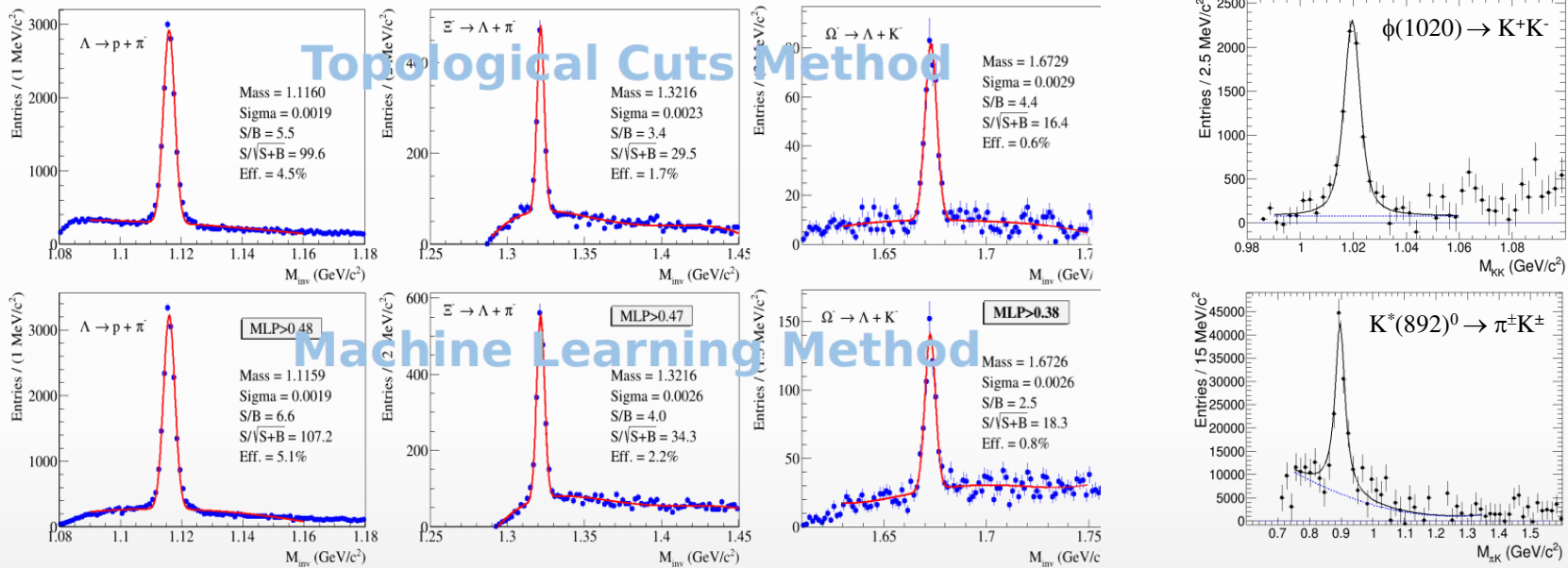
V. Vislavicius, A. Kalweit, arXiv:1610.03001



- ❖ System size scan for (multi)strange baryon and meson production is a key to understanding of strangeness production → unique capability of the MPD in the NICA energy range

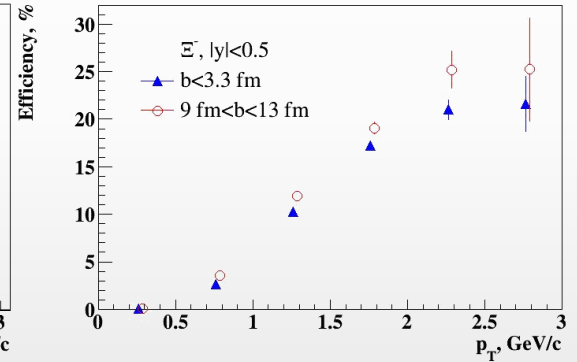
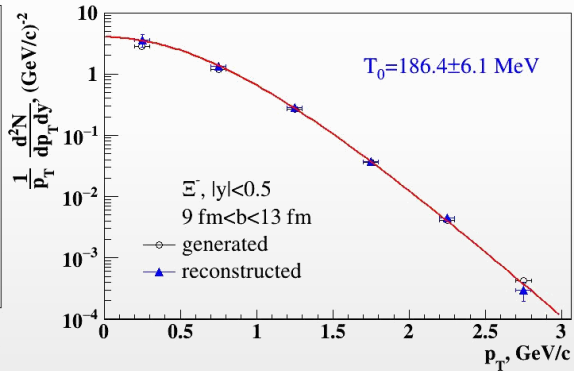
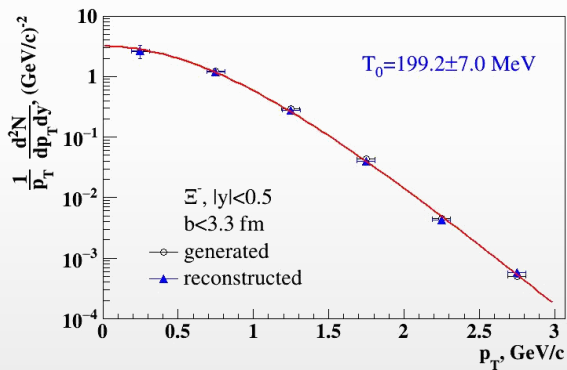
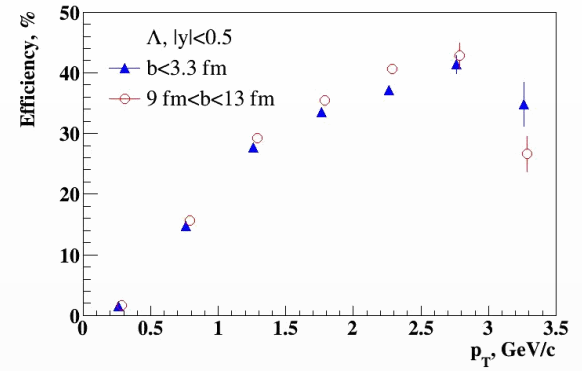
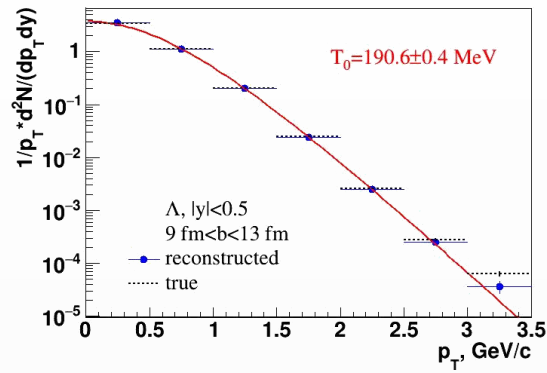
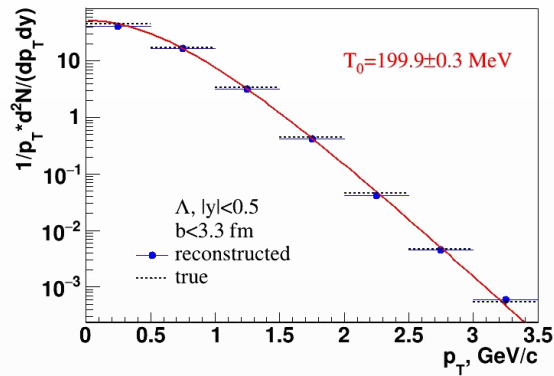


BiBi@9.2 GeV (UrQMD), 10 M events



Phys.Scripta 96 (2021) 6, 064002

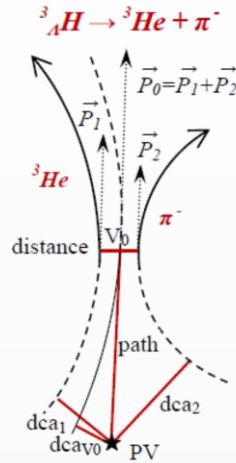
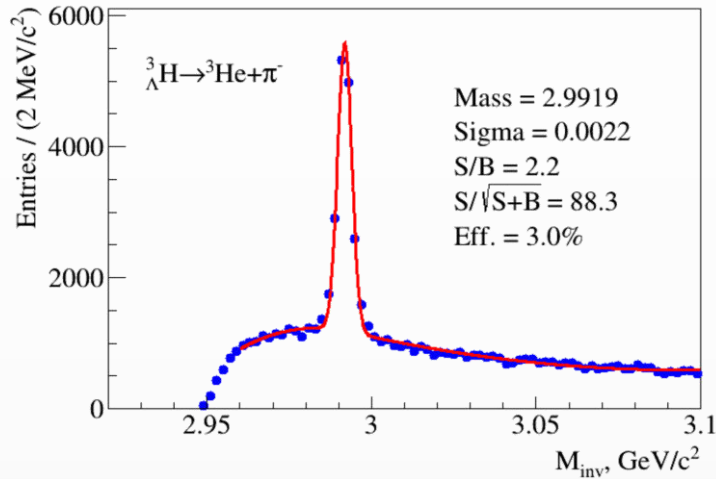
MPD has capabilities to measure production of charged  $\pi/K/p$ , (multi)strange baryons and resonances in pp, p-A and A-A collisions using charged hadron identification in the TPC&TOF and different decay topology selections



- ❖ Capability to reconstruct baryon yields down to low momenta with reasonable efficiencies
- ❖ High- $p_T$  reach is limited by statistics
- ❖ Reconstructed spectra are consistent with the generated ones  $\rightarrow$  MC closure test passed

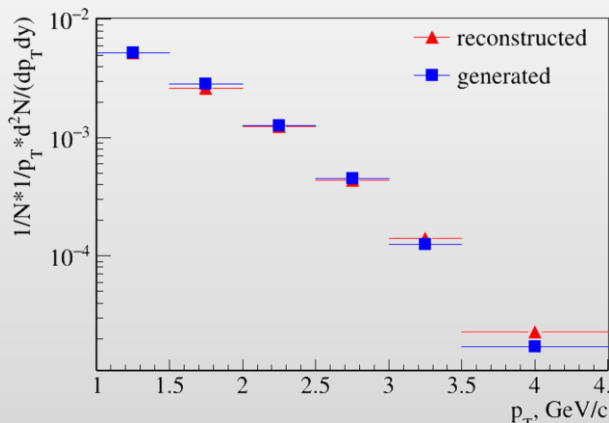
BiBi@9.2 GeV (PHQMD), 40 M events → full event/detector simulation and reconstruction

Phys.Part.Nucl.Lett. 19 (2022) 1, 46-53

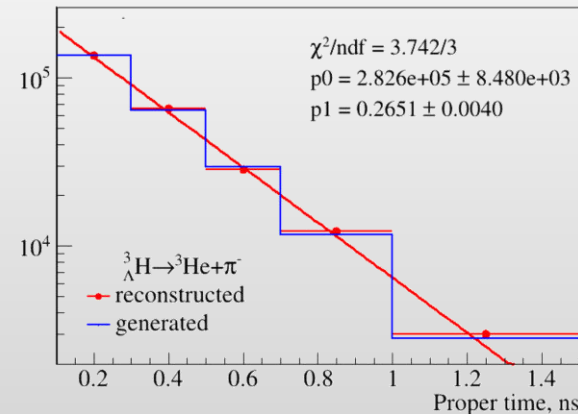


Decay channel	Branching ratio	Decay channel	Branching ratio
$\pi^- + {}^3\text{He}$	<b>24.7%</b>	$\pi^- + p + p + n$	1.5%
$\pi^0 + {}^3\text{H}$	12.4%	$\pi^0 + n + n + p$	0.8%
$\pi^- + p + d$	<b>36.7%</b>	$d + n$	0.2%
$\pi^0 + n + d$	18.4%	$p + n + n$	1.5%

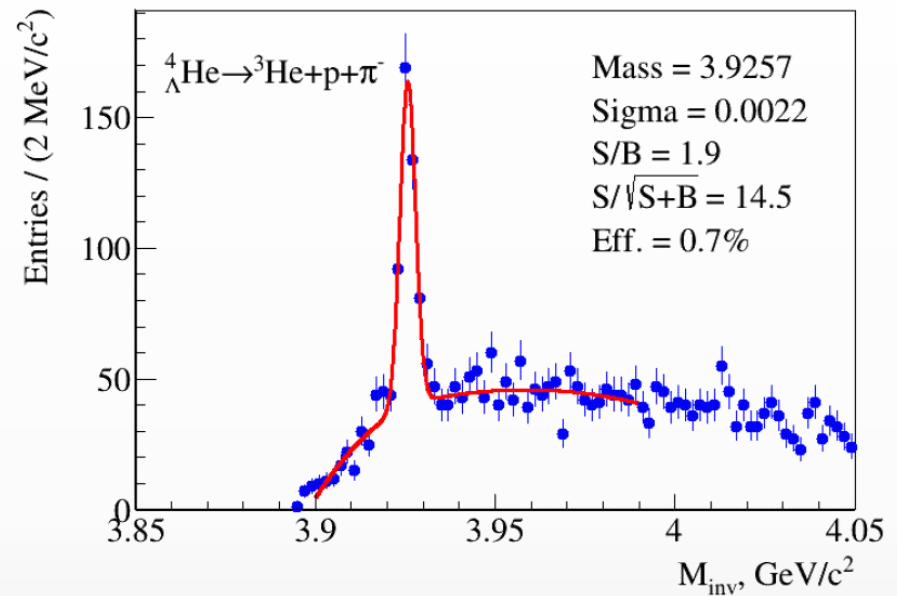
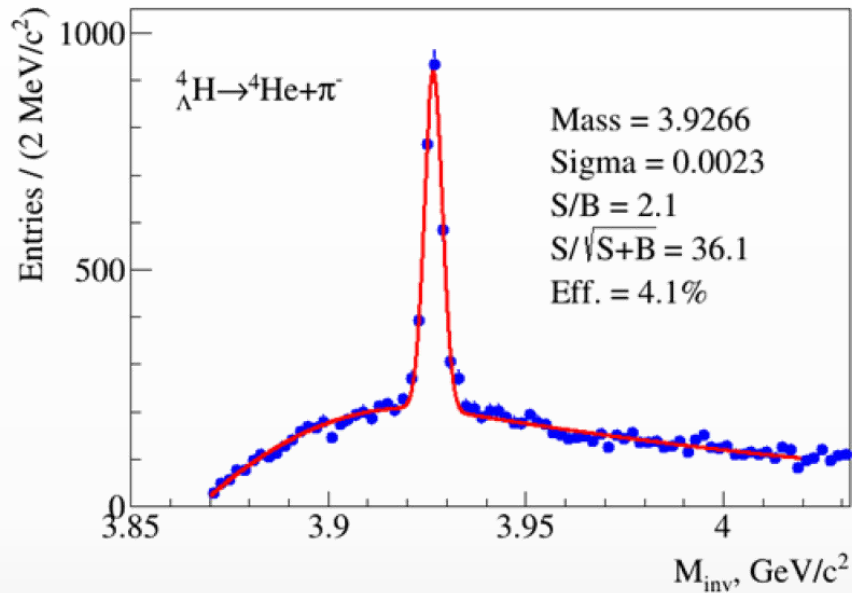
Spectrum is reconstructed up to  $p_T=4.5$  GeV/c



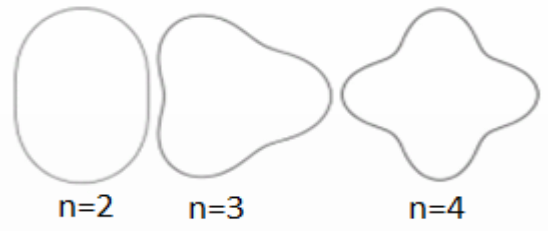
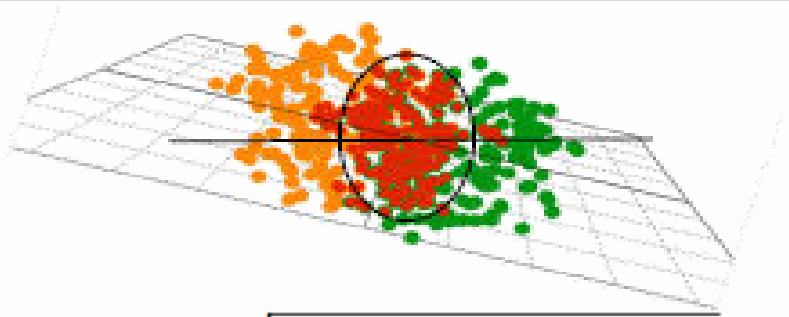
$$N(\tau) = N(0) \exp\left(-\frac{\tau}{\tau_0}\right) = N(0) \exp\left(-\frac{ML}{cp\tau_0}\right),$$



❖ First measurements for hypertriton will be possible with accumulation of ~ 50 M BiBi@9.2 events



- ❖ Monte Carlo events enriched with hypernuclei distributed by  $(\eta-p_T)$  phase space predicted by PHQMD
- ❖ Signals for heavier hypernuclei can be reconstructed with the equivalent statistics of  $\sim 140$  M events



$$\epsilon_n = \sqrt{\frac{\langle r^n \cos n\phi \rangle + \langle r^n \sin n\phi \rangle}{\langle r^n \rangle}}$$

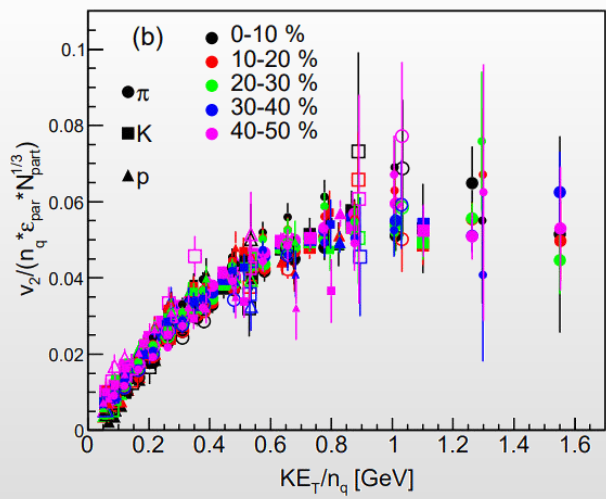
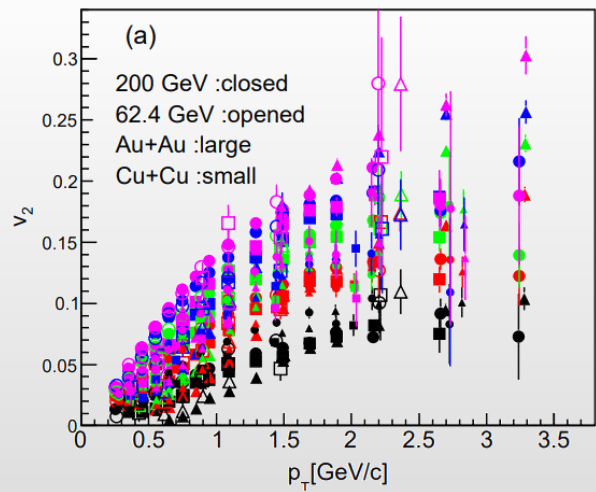
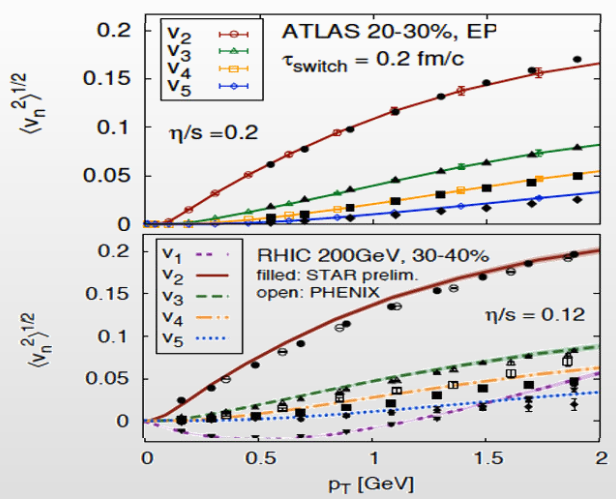


$$\frac{dN}{d\phi} \propto \left( 1 + 2 \sum_{n=1} v_n \cos [n(\phi - \Psi_n)] \right)$$

❖ Initial eccentricity and its fluctuations drive momentum anisotropy  $v_n$  with specific viscous modulation

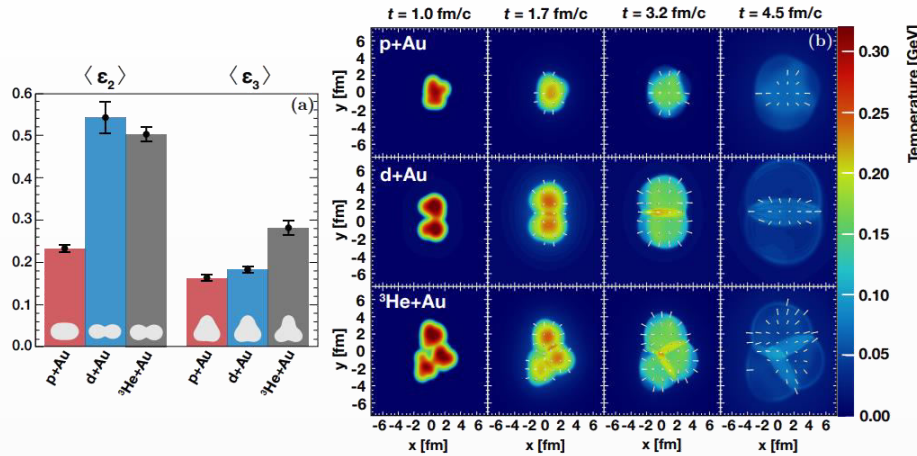
Gale, Jeon et al., Phys. Rev. Lett. 110, 012302

Phys.Rev.C 92 (2015) 3, 034913



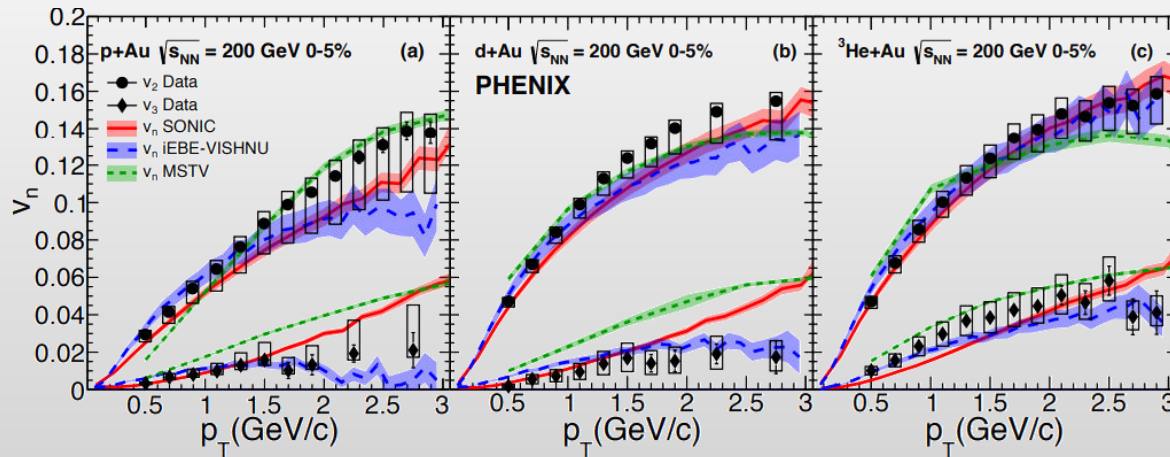
❖ Evidence for a dense perfect liquid found at RHIC/LHC (M. Roizard et al., Scientific American, 2006)

❖ System size scan (A-A) is an important part of systematic study (initial geometry → flow harmonics)

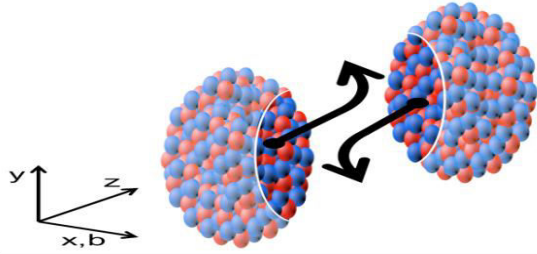


p-Au, d-Au and  $^3\text{He}$ -Au @ 200 GeV by PHENIX

- ❖ Measurements demonstrate that the  $v_n$ 's are correlated to the initial geometry
- ❖ Hydrodynamical models, which include the formation of a short-lived QGP droplet, provide a simultaneous description of these measurements

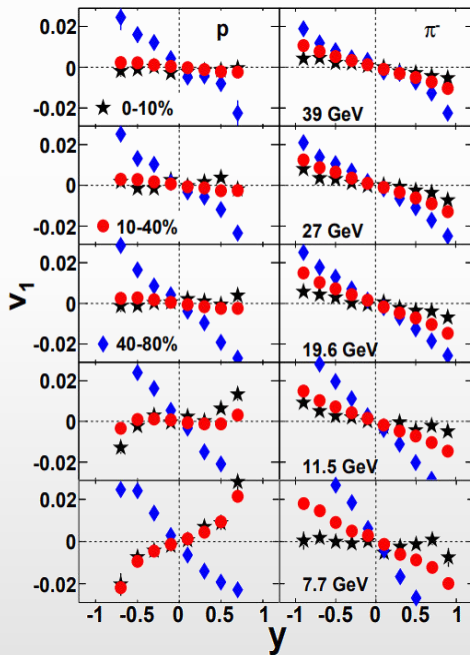


# Beam energy dependence



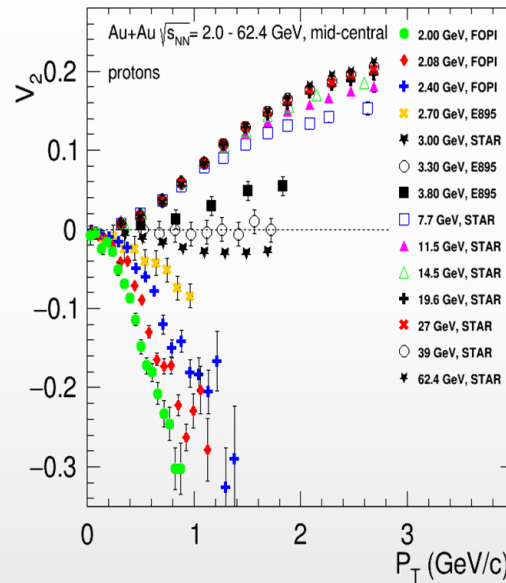
- ❖ Generated during the nuclear passage time  $(2R/\gamma)$  – sensitive to EOS
- ❖ RHIC @ 200 GeV  $(2R/\gamma) \sim 0.1$  fm/c
- ❖ AGS @ 3-4.5 GeV  $(2R/\gamma) \sim 9-5$  fm/c
- ❖  $v_1$  and  $v_2$  show strong centrality, energy and species dependence

Phys.Rev.Lett. 112 (2014) 16, 162301

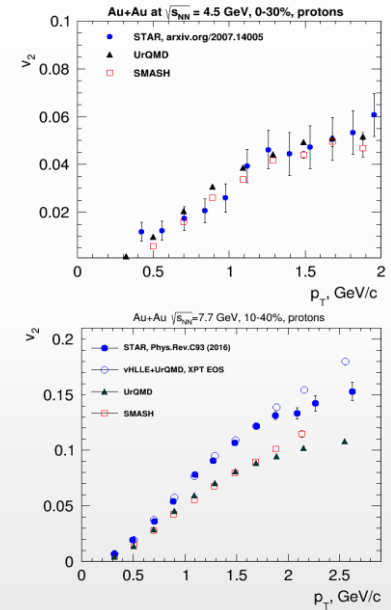


models do not reproduce measurements

EPJ Web Conf. 204 (2019) 03009



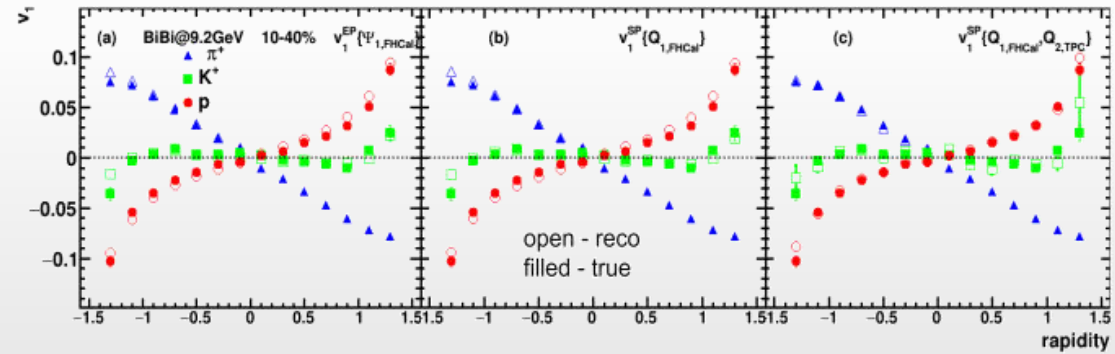
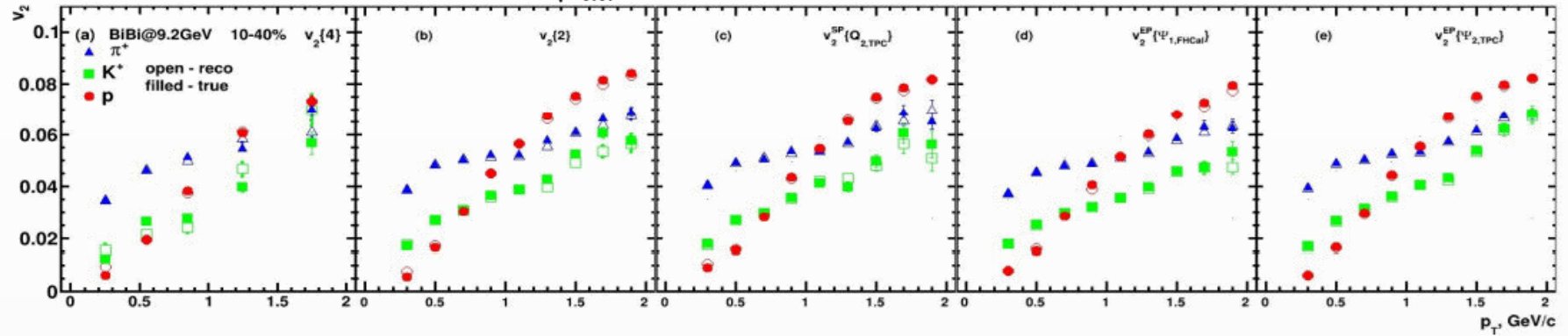
- ✓  $\sqrt{s_{NN}} \sim 3-4.5$  GeV, pure hadronic models reproduce  $v_2$  (JAM, UrQMD)  $\rightarrow$  degrees of freedom are the interacting baryons
- ✓  $\sqrt{s_{NN}} \geq 7.7$  GeV, need hybrid models with QGP phase (vHLLE+UrQMD, AMPT with string melting,...)



System size scan for flow measurements is vital for understanding of the medium transport properties and onset of the phase transition  $\rightarrow$  unique capability of the MPD in the NICA energy range

❖ UrQMD, BiBi@9.2 GeV

UrQMD, Bi+Bi,  $\sqrt{s_{NN}}=9.2$ , 10-40%, reconstructed (GEANT4) – production 25

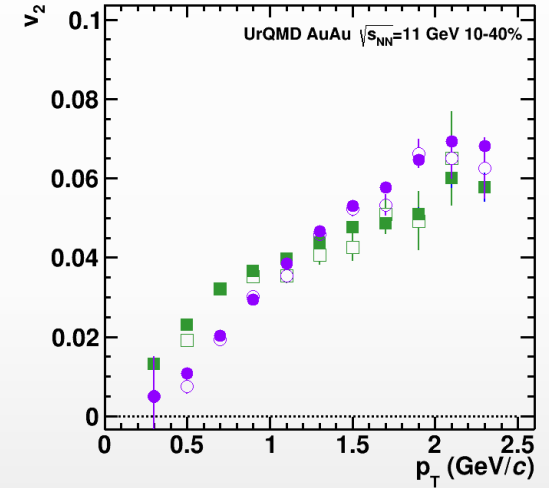
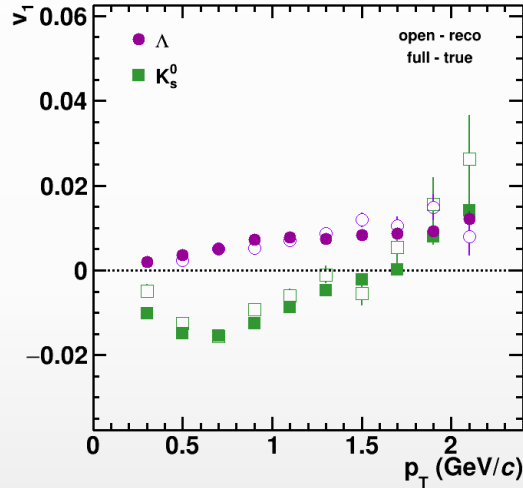
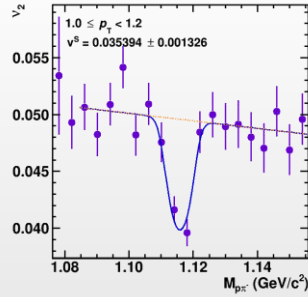
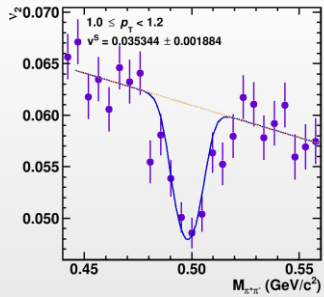
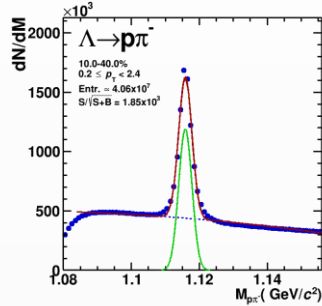
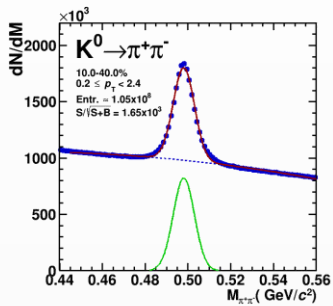


• Reconstructed and generated  $v_1$  and  $v_2$  for identified hadrons are in good agreement for all methods



AuAu@11 GeV (UrQMD), 25 M events  $\rightarrow$  full event/detector simulation and reconstruction

$$v_2^{SB}(\mathbf{m}_{inv}, \mathbf{p}_T) = v_2^S(\mathbf{p}_T) \frac{N^S(\mathbf{m}_{inv}, \mathbf{p}_T)}{N^{SB}(\mathbf{m}_{inv}, \mathbf{p}_T)} + v_2^B(\mathbf{m}_{inv}, \mathbf{p}_T) \frac{N^B(\mathbf{m}_{inv}, \mathbf{p}_T)}{N^{SB}(\mathbf{m}_{inv}, \mathbf{p}_T)}$$

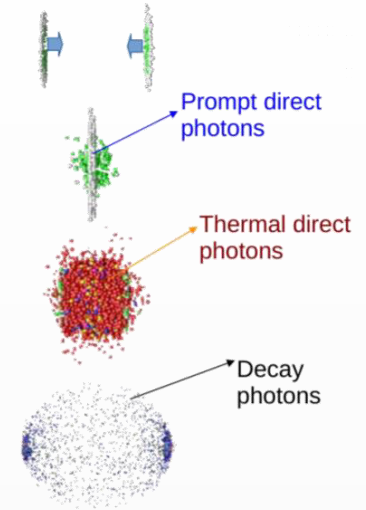


- ❖ Differential flow signal extraction using invariant mass fit method
- ❖ Reasonable agreement between reconstructed and generated  $v_n$  signals for  $K_S^0$  and  $\Lambda$

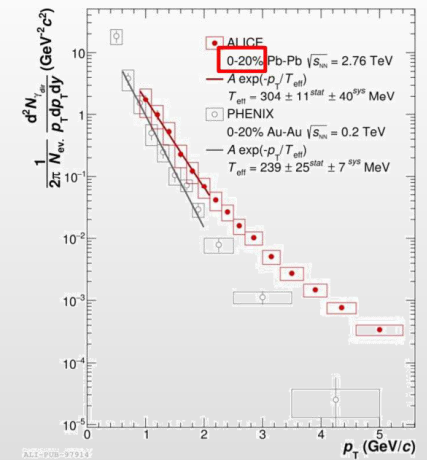
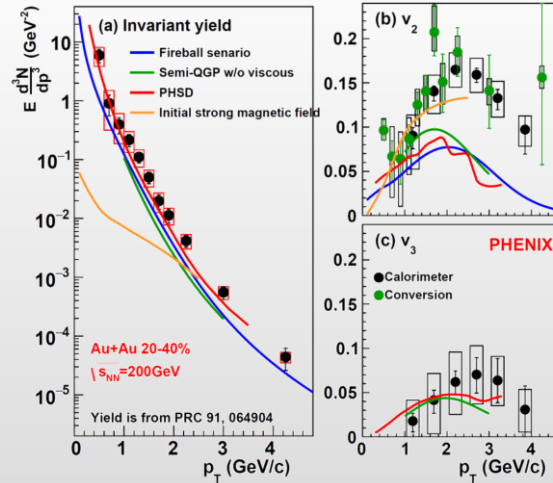
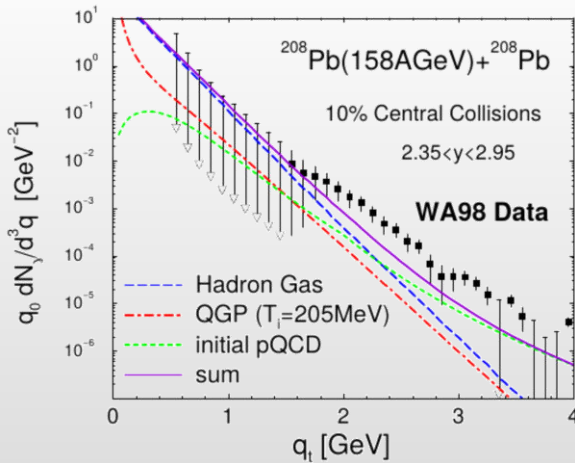
MPD has capabilities to measure different flow harmonics for a wide variety of identified hadrons in pp, p-A and A-A collisions

# Direct photons

- ❖ Direct photons – photons not from hadronic decays.
- ❖ Produced throughout the system evolution (thermal + prompt) :
  - ✓ penetrating probe
  - ✓ low-E - most direct estimation of the effective system temperature
  - ✓ high-E - hard scattering probe
- ❖ Direct photons in A-A collisions:
  - ✓ LHC, PbPb @ 2.76 and 5 TeV
  - ✓ RHIC, Au-Au(CuCu) @ 62-200 GeV
  - ✓ SPS, PbPb @ 17.2 GeV
- ❖ No measurements at NICA energies: yields and flow vs.  $p_T$  and centrality



Phys.Rev. C94 (2016) no.6, 064901



Simultaneous description of the large photon yields and flow is a challenge for theoretical models at RHIC and the LHC → “direct photon puzzle”

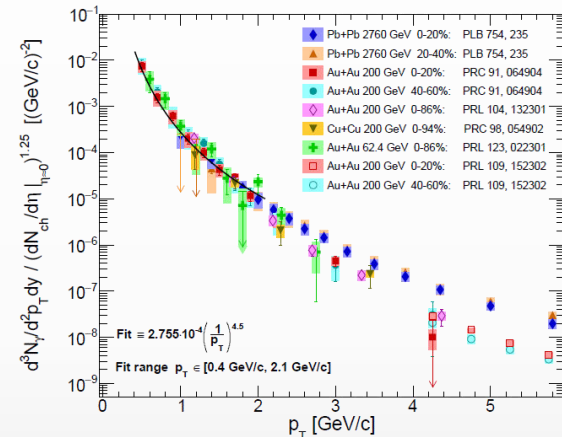
# Direct photon yields at NICA

Estimation of the direct photon yields @NICA

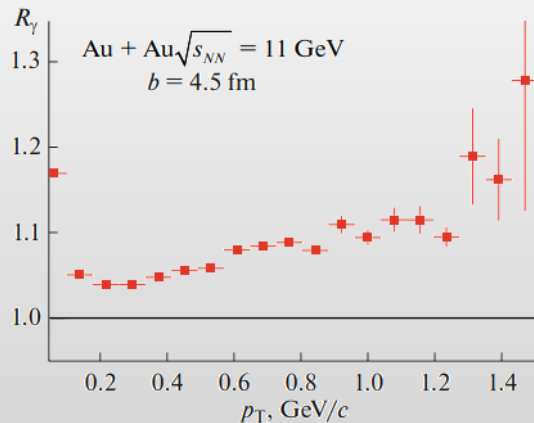
model  
calculations

empirical  
scaling

- ✓ UrQMD v3.4 with hybrid model (3+1D hydro, bag model EoS, hadronic rescattering and resonances within UrQMD)
- ✓ each cell have  $T_i, E_i, \mu_i$ :
  - $T$  is high – QGP phase (Peter Arnold, Guy D. Moore, Laurence G. Yaffe, JHEP 0112:009 2001)
  - $T$  is low – HG phase (Simon Turbide, Ralf Rapp, Charles Gale, Phys.Rev.C69:014903,2004)
  - $T$  is intermediate – mixed phase
- ✓ integrate over all cells and all time steps
- ✓ calculations reproduce hydro calculations for the SPS

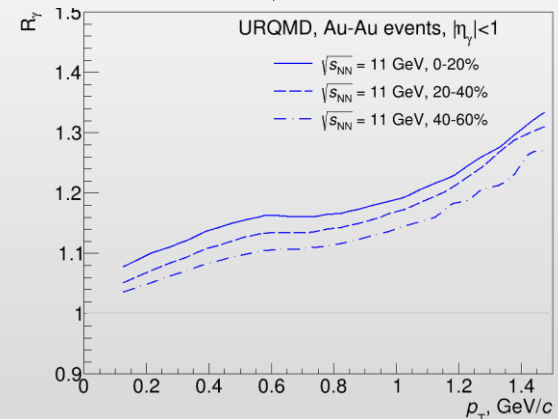


Physics of Particles and Nuclei, 2021, Vol. 52, No. 4, pp. 681–685



$$R_\gamma = \frac{\gamma_{\text{inc}}}{\gamma_{\text{decay}}} = \frac{\gamma_{\text{inc}}/\pi^0}{\gamma_{\text{decay}}/\pi^0_{\text{param}}}$$

$$\gamma_{\text{direct}} = \left(1 - \frac{1}{R_\gamma}\right) \cdot \gamma_{\text{inc}}$$

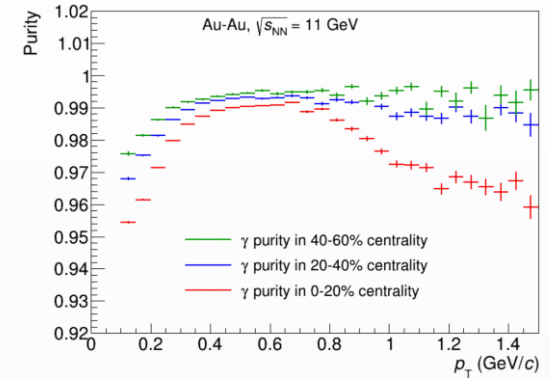
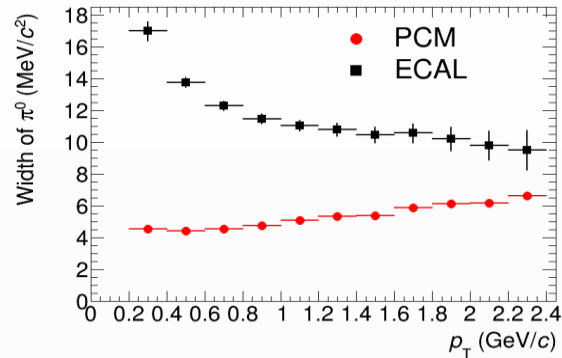
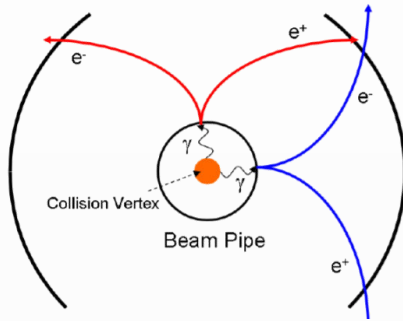


❖ Non-zero direct photon yields are predicted with  $R_\gamma \sim 1.05 - 1.15$  and  $v_2 \sim 0.5\%$  at top NICA energy

# Prospects for the MPD

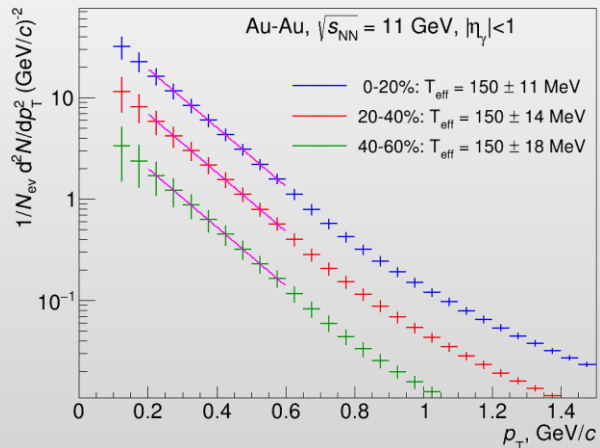
- ❖ Photons can be measured in the ECAL or in the tracking system as  $e^+e^-$  conversion pairs (PCM)

beam pipe (0.3%  $X_0$ ) + inner TPC vessels (2.4%  $X_0$ )



- ❖ Main sources of systematic uncertainties for direct photons:

- ✓ detector material budget  $\rightarrow$  conversion probability
- ✓  $\pi^0$  reconstruction efficiency
- ✓  $p_T$ -shapes of  $\pi^0$  and  $\eta$  production spectra



- ✓ ECAL and PCM for photon reconstruction and measurement of neutral mesons (background)
- ✓ With  $R_\gamma \sim 1.1$  and  $\delta R_\gamma/R_\gamma \sim 3\%$   $\rightarrow$  uncertainty of  $T_{\text{eff}} \sim 10\%$
- ✓ Development of reconstruction techniques and estimation of needed statistics are in progress

$\rightarrow$  potentially, MPD can provide unique measurements for direct photon production in the NICA energy range

# Multi-Purpose Detector (MPD) Collaboration



MPD International Collaboration was established in 2018 to construct, commission and operate the detector

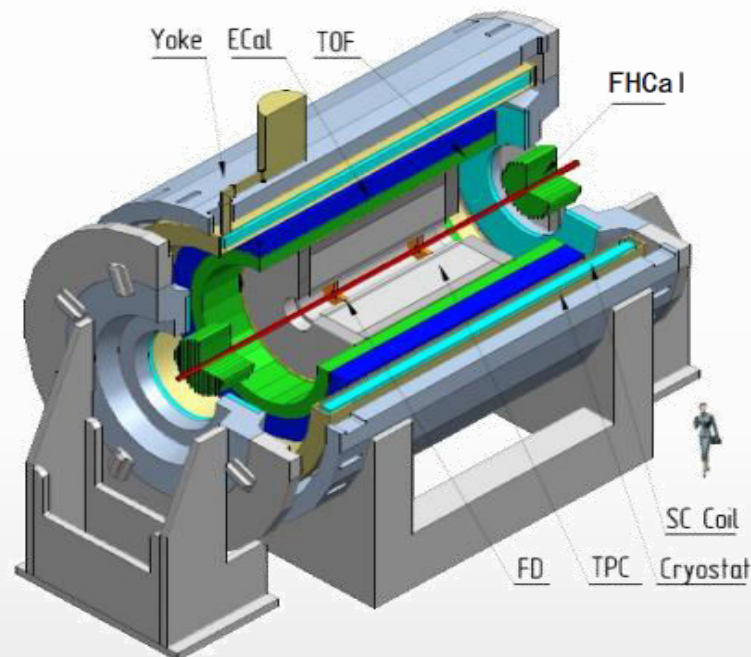
11 Countries, >500 participants, 35 Institutes and JINR

## Organization

Acting Spokesperson: **Victor Riabov**  
Deputy Spokespersons: **Zebo Tang, Arkadiy Taranenko**  
Institutional Board Chair: **Alejandro Ayala**  
Project Manager: **Slava Golovatyuk**

### Joint Institute for Nuclear Research;

A.Alikhanyan National Lab of Armenia, Yerevan, **Armenia**;  
University of Plovdiv, **Bulgaria**;  
Tsinghua University, Beijing, **China**;  
University of Science and Technology of China, Hefei, **China**;  
Huzhou University, Huzhou, **China**;  
Institute of Nuclear and Applied Physics, CAS, Shanghai, **China**;  
Central China Normal University, **China**;  
Shandong University, Shandong, **China**;  
University of Chinese Academy of Sciences, Beijing, **China**;  
University of South China, **China**;  
Three Gorges University, **China**;  
Institute of Modern Physics of CAS, Lanzhou, **China**;  
Tbilisi State University, Tbilisi, **Georgia**;  
Institute of Physics and Technology, Almaty, **Kazakhstan**;  
Benemérita Universidad Autónoma de Puebla, **Mexico**;  
Centro de Investigación y de Estudios Avanzados, **Mexico**;  
Instituto de Ciencias Nucleares, UNAM, **Mexico**;  
Universidad Autónoma de Sinaloa, **Mexico**;  
Universidad de Colima, **Mexico**;  
Universidad de Sonora, **Mexico**;  
Institute of Applied Physics, Chisinev, **Moldova**;  
Institute of Physics and Technology, **Mongolia**;



Belgorod National Research University, **Russia**;  
Institute for Nuclear Research of the RAS, Moscow, **Russia**;  
National Research Nuclear University MEPhI, Moscow, **Russia**;  
Moscow Institute of Science and Technology, **Russia**;  
North Osetian State University, **Russia**;  
National Research Center "Kurchatov Institute", **Russia**;  
Peter the Great St. Petersburg Polytechnic University Saint Petersburg, **Russia**;  
Plekhanov Russian University of Economics, Moscow, **Russia**;  
St.Petersburg State University, **Russia**;  
Skobeltsyn Institute of Nuclear Physics, Moscow, **Russia**;  
Petersburg Nuclear Physics Institute, Gatchina, **Russia**;  
Vinča Institute of Nuclear Sciences, **Serbia**;  
Pavol Jozef Šafárik University, Košice, **Slovakia**



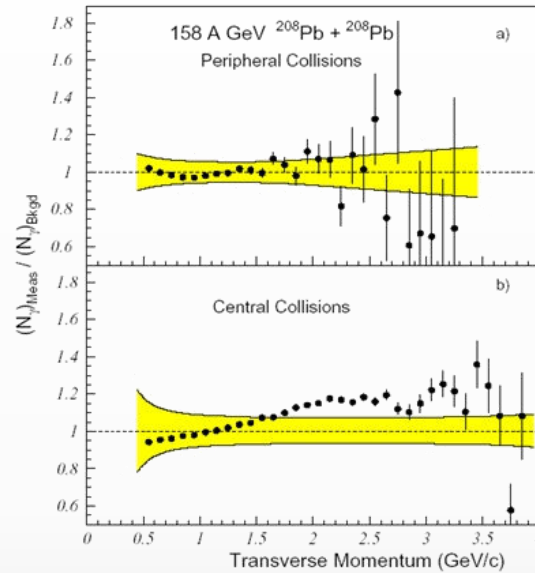
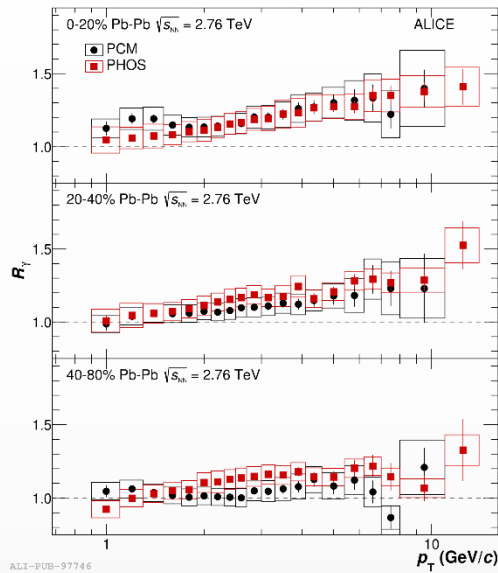


- ❖ MPD is approaching its commissioning in 2025
- ❖ MPD has a solid physics program and can potentially provide unique results on the structure of the QCD phase diagram, provide insight into inner structure of compact star and neutron star mergers

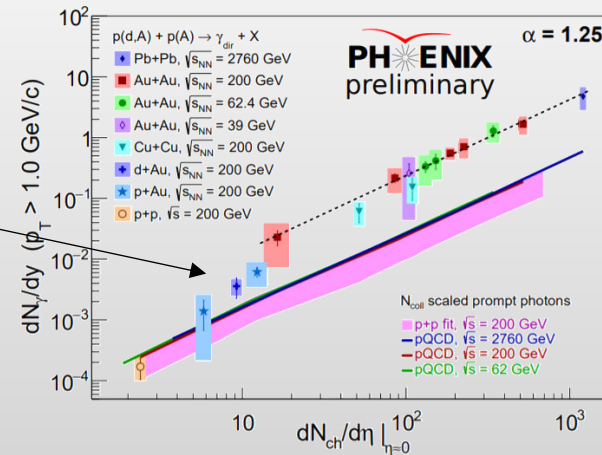
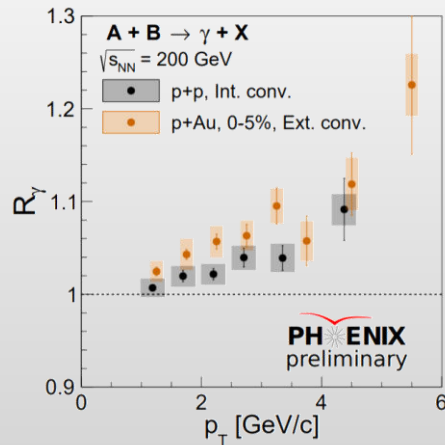
# BACKUP

# Comparison to higher energies

- $R_\gamma \sim 1.05-1.2$  in heavy-ion collisions at SPS/RHIC/LHC,  $\sqrt{s_{NN}} = 17.2-2760$  GeV



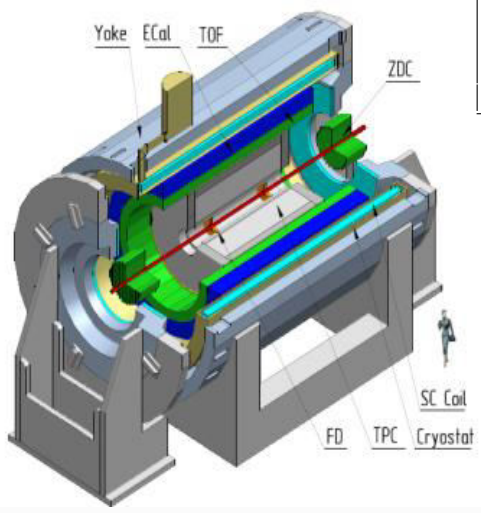
- $R_\gamma \sim 1.05$  is on the verge of experimental measurability (PHENIX in pp/pA@200,  $\geq 2\sigma$ )





# Multi-Purpose Detector

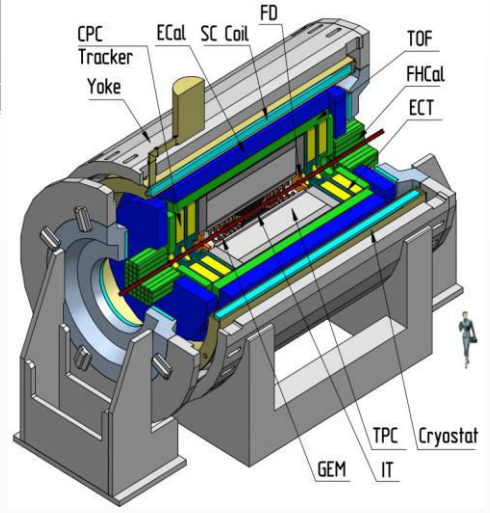
## Stage- I



Length	340 cm
Vessel outer radius	140 cm
Vessel inner radius	27 cm
Default magnetic field	0.5 T
Drift gas mixture	90% Ar+10% CH <sub>4</sub>
Maximum event rate	7 kHz ( $L = 10^{27} \text{ cm}^{-2}\text{s}^{-1}$ )



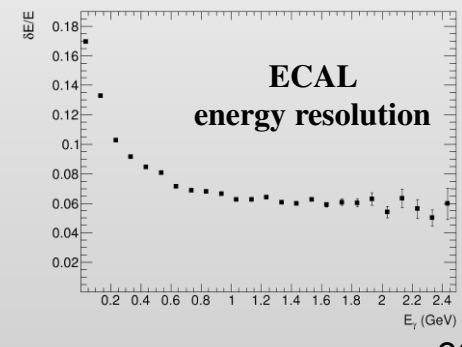
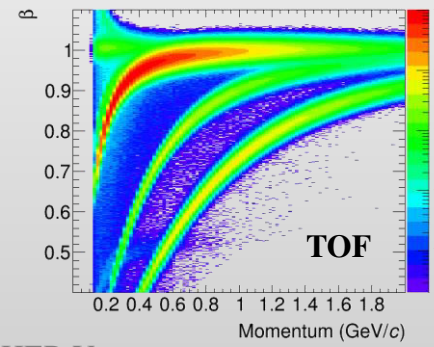
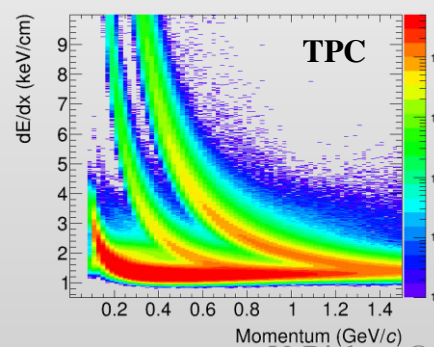
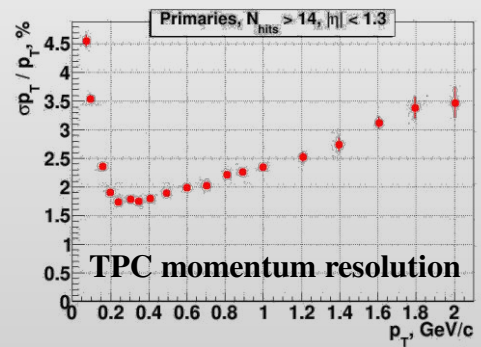
## Stage- II



- TPC:**  $|\Delta\phi| < 2\pi, |\eta| \leq 1.6$
- TOF, EMC:**  $|\Delta\phi| < 2\pi, |\eta| \leq 1.4$
- FFD:**  $|\Delta\phi| < 2\pi, 2.9 < |\eta| < 3.3$
- FHCAL:**  $|\Delta\phi| < 2\pi, 2 < |\eta| < 5$

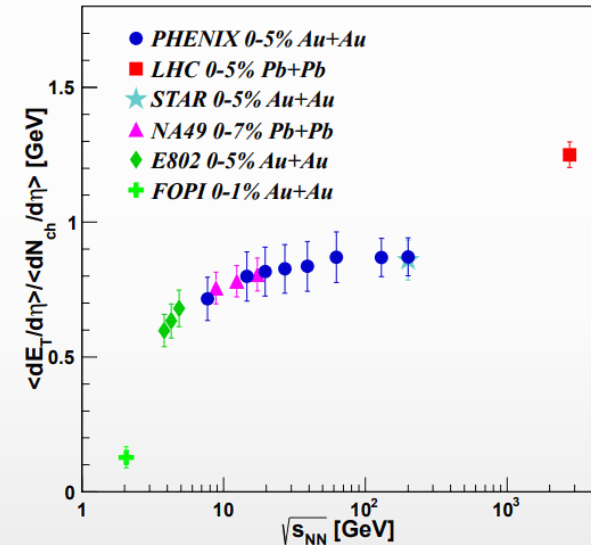
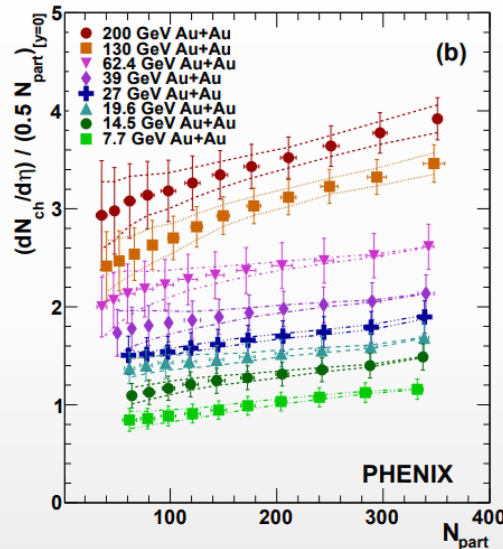
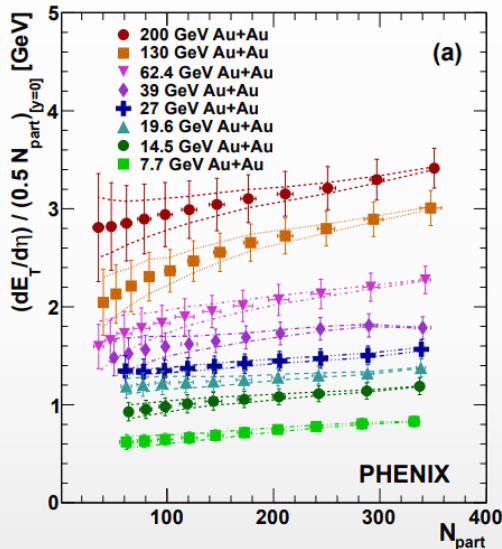
- + ITS** (heavy-flavor measurements)
- + forward spectrometers**

Au+Au @ 11 GeV (UrQMD + full chain reconstruction)



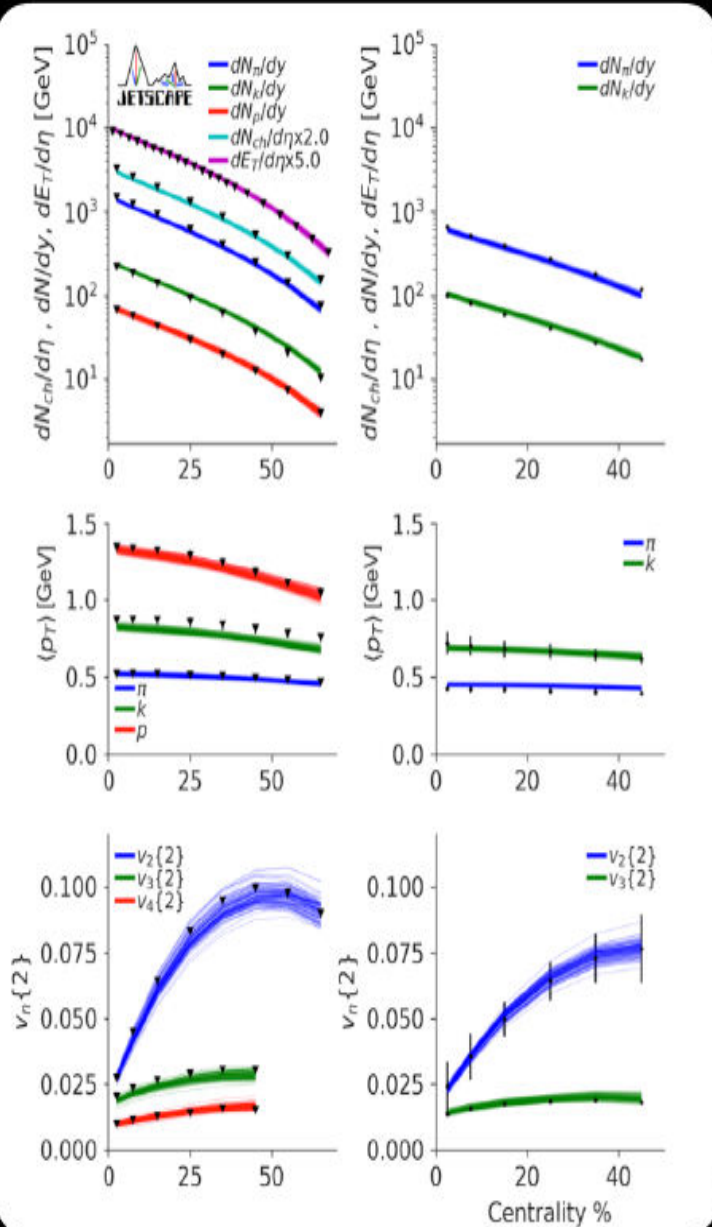
- ❖ Transverse energy and charged-particle multiplicity provide characterization of the nuclear geometry of the reaction, sensitive to dynamics of the colliding system (centrality, energy density, etc.)
- ❖  $E_T/N_{ch}$  at NICA shows a quick increase of the average transverse mass of the produced particles

Phys.Rev.C 93 (2016) 2, 024901



- ❖ Many references for cross-checks with other experiments
- ❖ The measurements will constitute the first physics results from the MPD

# GLOBAL BAYESIAN CONSTRAINTS ON QGP VISCOSITY



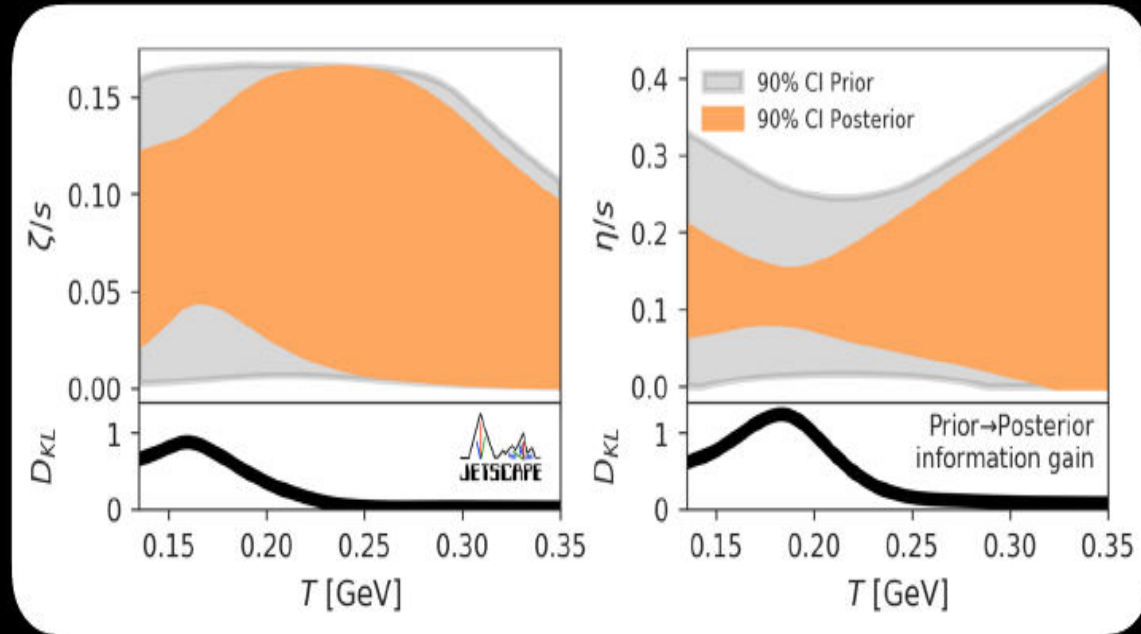
S. Pratt, E. Sangaline, P. Sorensen and H. Wang, Phys. Rev. Lett. 114, 202301 (2015)

J. E. Bernhard, J. S. Moreland, S. A. Bass, J. Liu and U. Heinz, Phys. Rev. C94, 024907 (2016)

J. E. Bernhard, J. S. Moreland and S. A. Bass, Nature Phys. 15, 1113-1117 (2019)

G. Nijs, W. Van Der Schee, U. Gürsoy and R. Snellings, Phys. Rev. Lett. 126, 202301 (2021) & Phys. Rev. C103, 054909 (2021)

D. Everett *et al.* [JETSCAPE], Phys. Rev. Lett. 126, 242301 & Phys. Rev. C103, 054904 (2021)



- Precision hadronic measurements can systematically constrain the QGP viscosity

# Elliptic flow measurements using TPC: Scalar product, Event-plane

$$u_2 = \cos 2\phi + i \sin 2\phi = e^{2i\phi}$$

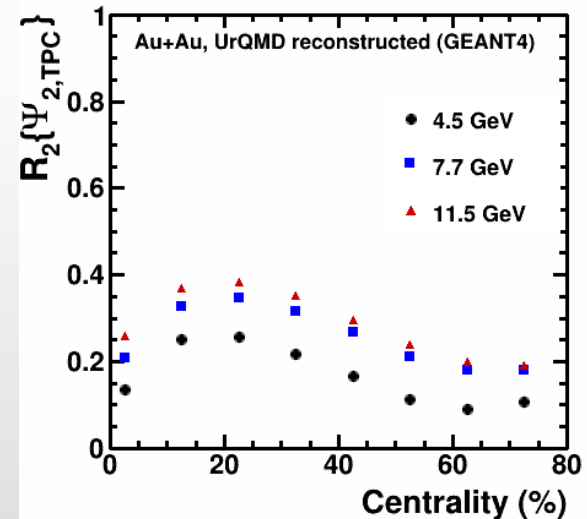
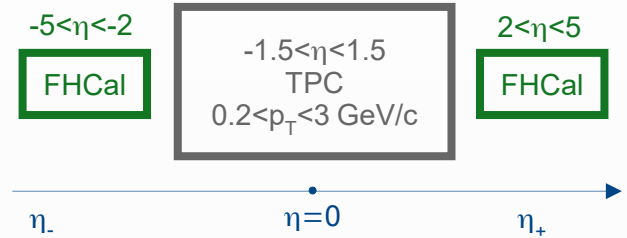
$$Q_2 = \sum_{j=1}^M \omega_j u_{2,j}, \quad \Psi_{2,\text{TPC}} = \frac{1}{2} \tan^{-1} \left( \frac{Q_{2,y}}{Q_{2,x}} \right)$$

- **Scalar product:**  $v_2^{\text{SP}} \{Q_{2,\text{TPC}}\} = \frac{\langle u_{2,\eta\pm} Q_{2,\eta\mp}^* \rangle}{\sqrt{\langle Q_{2,\eta+} Q_{2,\eta-} \rangle}}$

- **TPC Event-plane:**

$$v_2^{\text{EP}} \{\Psi_{2,\text{TPC}}\} = \frac{\langle \cos [2(\phi_{\eta\pm} - \Psi_{2,\eta\mp})] \rangle}{R_2^{\text{EP}} \{\Psi_{2,\text{TPC}}\}}$$

$$R_2^{\text{EP}} \{\Psi_{2,\text{TPC}}\} = \sqrt{\langle \cos [2(\Psi_{2,\eta+} - \Psi_{2,\eta-})] \rangle}$$

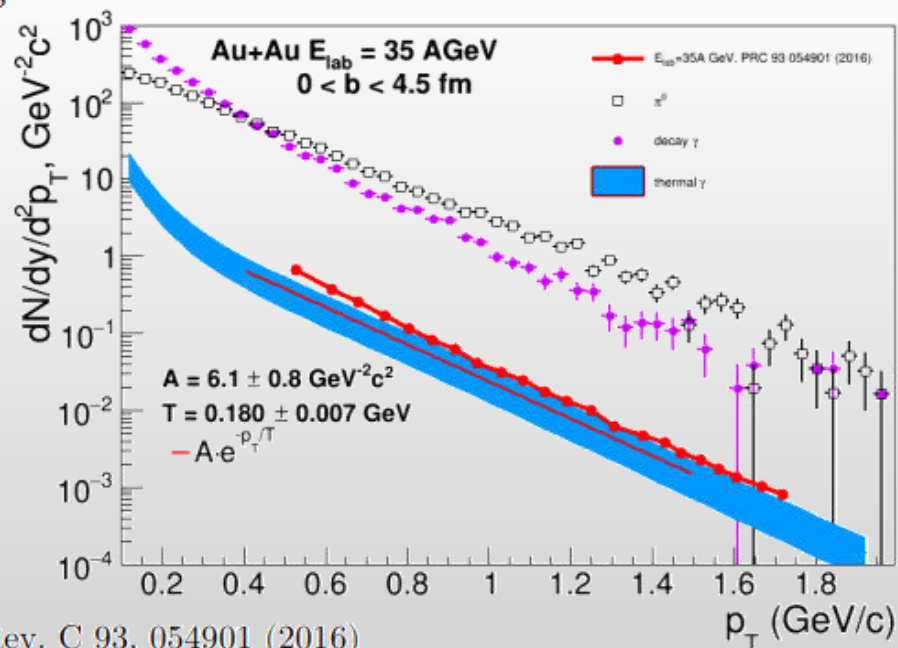


# Simulation setup

- ✓ UrQMD v3.4 with hybrid model (3+1d hydro, **bag model** EoS, hadronic rescattering and resonances within UrQMD)
- ✓  $\pi^0$  and decay photon spectrum are calculated **within the same simulation**
- ✓ impact parameter range  $0 < b < 9$  fm
- ✓ In hydrodynamical evolution, for each volume we calculate thermal gamma yield based on  $T$ , energy density ( $e$ ), QGP fraction, baryonic chemical potential. We integrate these yields over time (until freeze-out time) and space.
- ✓ Two extreme cases: calculate thermal gamma emission from the volume above freeze-out criterion ( $e > e_{\text{freezeout}}$ ), or calculate for all volumes. Reality somewhere in between (all volumes interact during hydro evolution). Comparing these options one can estimate theoretical uncertainties

$$\frac{d^3 N^{\gamma, \text{therm}}}{dy d^2 k_T} = \int_{\Omega} dV dt R_{\gamma}(k, T(x), \mu(x), u(x))$$

Why simulations in PRC 93 054901 (2016) and PRC 81 044904 (2010) have almost the same yield despite ~5 times difference in energy (35 vs 158 AGeV)?



# Finite-Size Effects and search for CEP

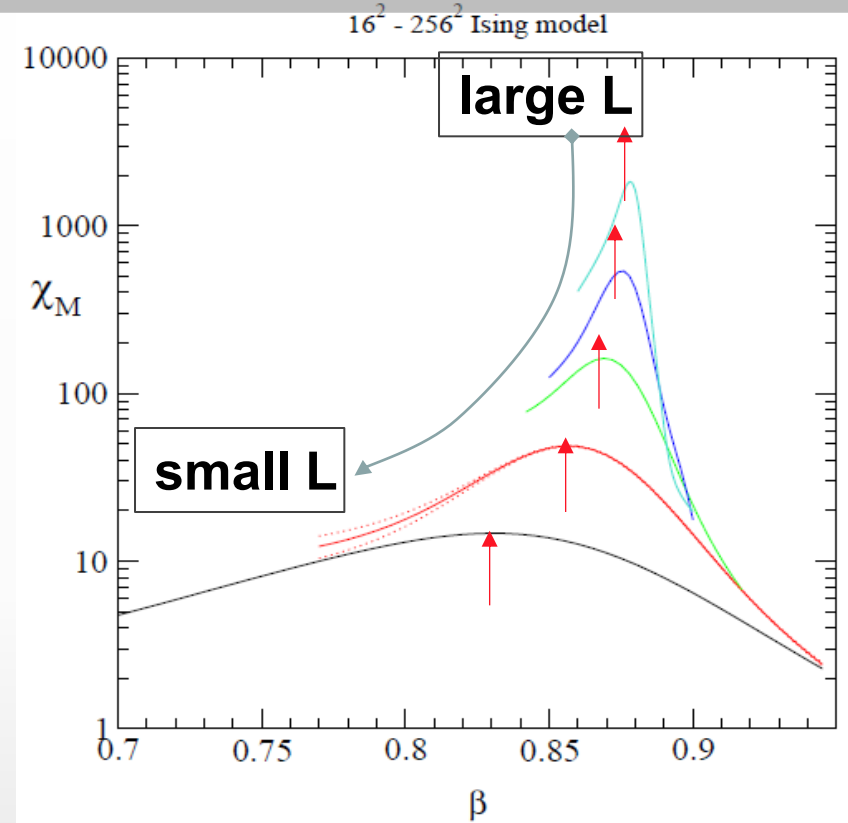
In HIC, both the size ( $L$ ) and duration of formed system are finite.

## Critical behavior changes with $L$

If the  $L$  is too small, the correlation length  $\xi$  can not be fully developed to cause a phase transition.

if the correlation length  $\xi \sim |T - T_c|^{-\nu} \leq L$  the finite-size effect is not negligible and only a **pseudo-critical point, shifted from the genuine CEP, is observed.**

- ✓ Finite-size effects have a specific dependencies on size ( $L$ )
- ✓ The scaling of these dependencies give access to the CEP's location, it's critical exponents and scaling function.



Note change in peak heights positions & widths with  $L$

❖ Data taking by STAR at RHIC:  $3 < \sqrt{s_{NN}} < 200$  GeV ( $750 < \mu_B < 25$  MeV)

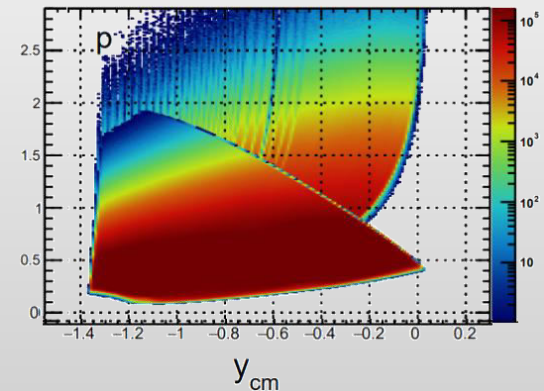
Au+Au Collisions at RHIC											
Collider Runs						Fixed-Target Runs					
	$\sqrt{s_{NN}}$ (GeV)	#Events	$\mu_B$	$y_{beam}$	run		$\sqrt{s_{NN}}$ (GeV)	#Events	$\mu_B$	$y_{beam}$	run
1	200	380 M	25 MeV	5.3	Run-10, 19	1	13.7 (100)	50 M	280 MeV	-2.69	Run-21
2	62.4	46 M	75 MeV		Run-10	2	11.5 (70)	50 M	320 MeV	-2.51	Run-21
3	54.4	1200 M	85 MeV		Run-17	3	9.2 (44.5)	50 M	370 MeV	-2.28	Run-21
4	39	86 M	112 MeV		Run-10	4	7.7 (31.2)	260 M	420 MeV	-2.1	Run-18, 19, 20
5	27	585 M	156 MeV	3.36	Run-11, 18	5	7.2 (26.5)	470 M	440 MeV	-2.02	Run-18, 20
6	19.6	595 M	206 MeV	3.1	Run-11, 19	6	6.2 (19.5)	120 M	490 MeV	1.87	Run-20
7	17.3	256 M	230 MeV		Run-21	7	5.2 (13.5)	100 M	540 MeV	-1.68	Run-20
8	14.6	340 M	262 MeV		Run-14, 19	8	4.5 (9.8)	110 M	590 MeV	-1.52	Run-20
9	11.5	157 M	316 MeV		Run-10, 20	9	3.9 (7.3)	120 M	633 MeV	-1.37	Run-20
10	9.2	160 M	372 MeV		Run-10, 20	10	3.5 (5.75)	120 M	670 MeV	-1.2	Run-20
11	7.7	104 M	420 MeV		Run-21	11	3.2 (4.59)	200 M	699 MeV	-1.13	Run-19
						12	3.0 (3.85)	2000 M	750 MeV	-1.05	Run-18, 21

❖ A very impressive and successful program with many collected datasets, already available and expected results

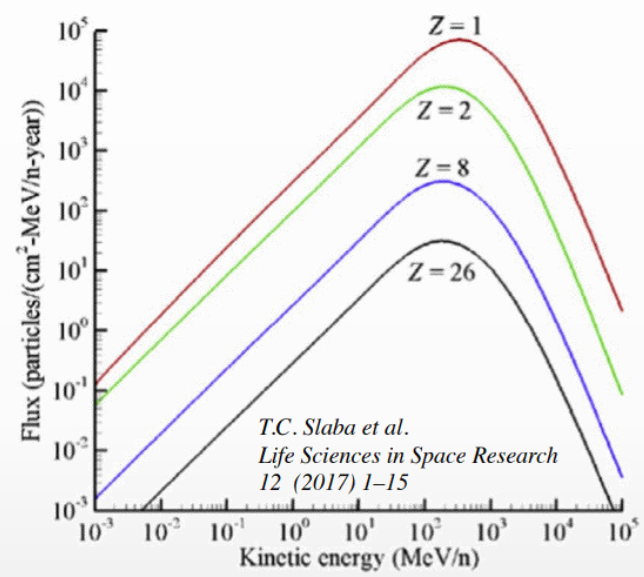
❖ Limitations:

- ✓ Au+Au collisions only
- ✓ Among the fixed-target runs, only the 3 GeV data have full mid-rapidity coverage for protons ( $|y| < 0.5$ ), which is crucial for physics observables

Au+Au @ 3.9 GeV



- ❖ Galactic Cosmic Rays composed of nuclei (protons, ... up to Fe) and E/A up to 50 GeV
- ❖ These high-energy particles create cascades of hundreds of secondary, etc. particles

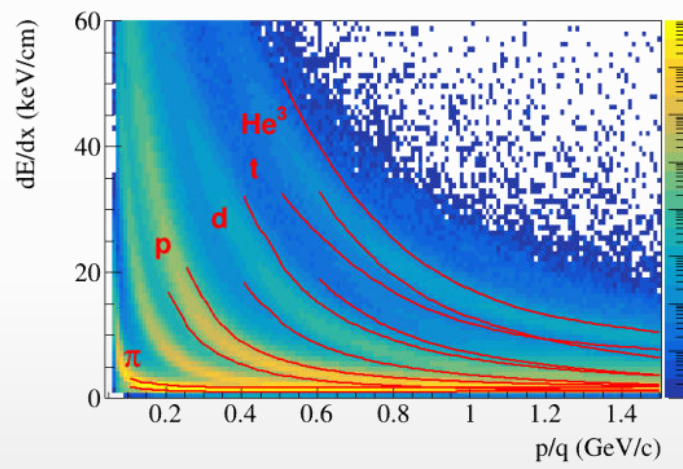


- ❖ Cosmic rays are a serious concern to astronauts, electronics, and spacecraft.
- ❖ The damage is proportional to  $Z^2$ , therefore the component due to ions is important
- ❖ Damage from secondary production of p, d, t,  $^3\text{He}$ , and  $^4\text{He}$  is also significant
- ❖ Need input information for transport codes for shielding applications (Geant-4, Fluka, PHITS, etc.):
  - ✓ total, elastic/reaction cross section
  - ✓ particle multiplicities and coelcense parameters
  - ✓ outgoing particle distributions:  $d^2N/dE d\Omega$

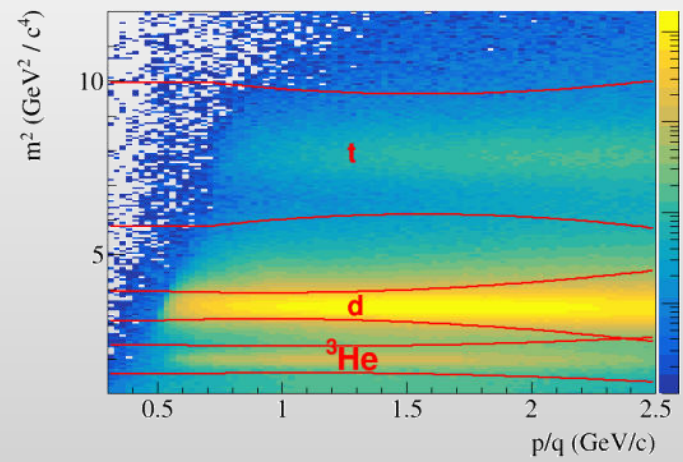
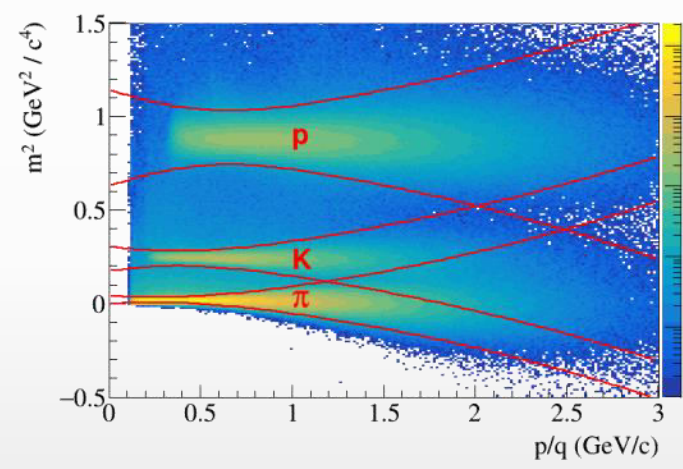


- ❖ NICA can deliver different ion beam species and energies:
  - ✓ Targets of interest (C = astronaut, Si = electronics, Al = spacecraft) + He, C, O, Si, Fe, etc.
- ❖ No data exist for projectile energies > 3 GeV/n

dE/dx vs momentum in TPC



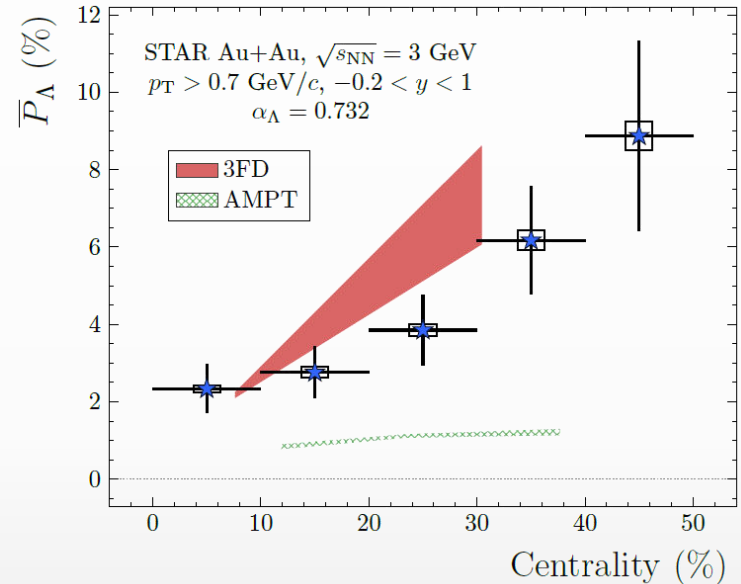
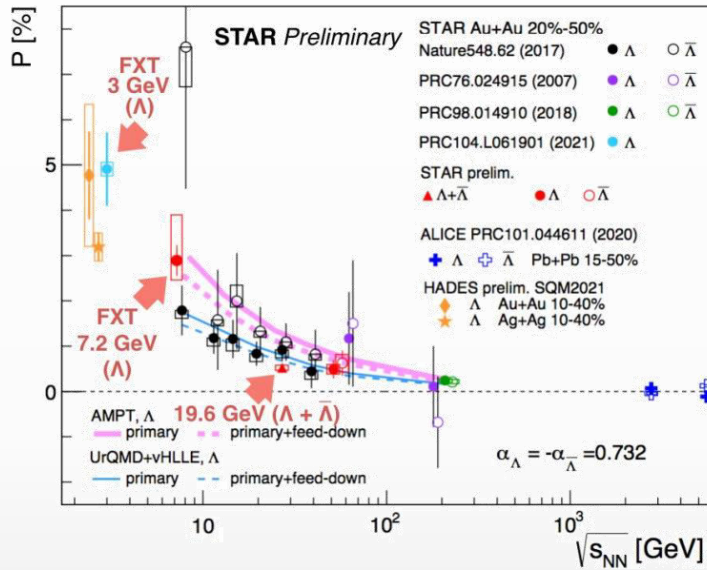
$m^2$  vs. momentum in TOF



MPD has excellent light fragment identification capabilities in a wide rapidity range → unique capability of the MPD in the NICA energy range

❖ Global hyperon polarization measurements in mid-central A+A collisions at  $\sqrt{s_{NN}} = 3-5000$  GeV

STAR, Phys.Rev.C, 104(6):L061901, 2021



- ❖ Global polarization of hyperons experimentally observed, decreases with  $\sqrt{s_{NN}}$
- ❖ Hint for a  $\Lambda - \bar{\Lambda}$  difference, magnetic field,  $P_\Lambda \simeq \frac{1}{2} \frac{\omega}{T} + \frac{\mu_\Lambda B}{T}$ ,  $P_{\bar{\Lambda}} \simeq \frac{1}{2} \frac{\omega}{T} - \frac{\mu_\Lambda B}{T}$  ?
- ❖ Feed down from  $\Sigma(1385) \rightarrow \Lambda\pi$ ,  $\Sigma^0 \rightarrow \Lambda\gamma$ ;  $\Xi \rightarrow \Lambda\pi$  reduces polarization by  $\sim 10-20\%$
- ❖ Energy dependence of global polarization is reproduced by AMPT, 3FD, UrQMD+vHLLLE
- ❖ AMPT with partonic transport strongly underestimates measurements at  $\sqrt{s_{NN}} = 3$  GeV  $\rightarrow$  hadron gas?

MPD: extra points in the energy range 3-10 10 GeV with small uncertainties; centrality,  $p_T$  and rapidity dependence of polarization not only for  $\Lambda$ , but other (anti)hyperons ( $\Lambda$ ,  $\Sigma$ ,  $\Xi$ )